Engineering Structures 225 (2020) 111243

Contents lists available at ScienceDirect

Engineering Structures

journal homepage: www.elsevier.com/locate/engstruct

Seismic retrofit of existing school buildings in Italy: Performance evaluation and loss estimation

Wilson Carofilis[a,*], Daniele Perrone[a], Gerard J. O'Reilly[a], Ricardo Monteiro[a], Andre Filiatrault[a,b]

[a] University School for Advanced Studies IUSS Pavia, Italy
[b] Department of Civil, Structural, and Environmental Engineering, State University of New York at Buffalo, NY 14260, USA

ARTICLE INFO

Keywords:
Performance assessment
Seismic retrofit
Cost-benefit analysis
Loss estimation
Failure mechanism

ABSTRACT

The seismic vulnerability and inadequate behaviour of existing school buildings observed during past earthquakes in Italy have raised awareness of the need to upgrade their performance. This paper examines different retrofit strategies for three case study school buildings, representing the main typologies found within the Italian school building stock. The three building typologies investigated in this study are representative of reinforced concrete (RC), precast concrete (PC) and unreinforced masonry (URM) school buildings. A seismic performance assessment was carried out using detailed numerical models that consider the main structural deficiencies documented for older buildings in Italy, generally designed and built before the 1970s. The retrofit interventions were specifically aimed at mitigating these main structural deficiencies in order to meet current building code limit state requirements. These requirements are set to limit the damage to non-structural elements and prevent non-ductile failure mechanisms in the structural system, following a typical building code and practitioner-oriented process. The retrofit alternatives were then evaluated through increasing ground shaking intensities to quantify risk-based decision variables, such as the expected annual loss and mean annual frequency of collapse. The results highlight the level of adequacy of each retrofit option in reducing both the economic losses and collapse vulnerability. To predict the economic feasibility of these interventions, a cost-benefit analysis was also conducted using estimated implementation costs of each retrofit alternative. Lastly, the results were also compared with the outcome of the seismic risk classification guidelines, recently proposed in Italy.

1. Introduction

Extensive damage and structural collapse observed in Italian school buildings during past seismic events have pointed out the need for seismic risk mitigation programmes. These should identify the most vulnerable building typologies and reduce the earthquake-related economic losses and casualties through adequate seismic retrofit strategies. The collapse of a school in San Giuliano di Puglia during the 2002 Molise earthquake in Italy, which caused 30 fatalities, is a key example of the seismic vulnerability of the Italian existing school building stock [1]. Recent studies have also pointed out the importance of non-structural elements in achieving adequate seismic performance levels for an entire building system [2–4]. De Angelis and Pecce [5] reported the death of a student caused by the collapse of a classroom ceiling on November 22nd, 2008 at the Darwin High School in Rivoli, Italy and proposed a simplified methodology to assess the safety of non-structural elements installed in school buildings. Based on these considerations, the need for a seismic risk identification scheme for Italian school buildings comprising both structural and non-structural elements, along with the definition of the seismic retrofit strategies appears evident. Grant et al. [6] developed a risk-management framework to prioritise rehabilitation interventions for Italian school buildings; once the more vulnerable structures are identified, adequate and/or practical retrofitting techniques can then be proposed. Calvi [7] described appropriate strengthening intervention strategies that logically employ available resources. A cost-benefit analysis, using the breakeven time as metric, is a useful tool to understand whether or not a retrofit strategy is feasible from an economical point of view, as studied by Cardone et al. [8]. Furthermore, the seismic risk classification guidelines recently introduced in Italy [9] provide a simplified method that classifies existing buildings before and after strengthening interventions. The use of these guidelines may result in tax deductions as an incentive to improve the seismic safety of the existing Italian school building stock, leading to increased awareness of seismic safety and the importance of adequate seismic retrofit among citizens.

To contribute to this important issue, the European Centre for

* Corresponding author.
E-mail address: wilson.carofilis@iusspavia.it (W. Carofilis).

https://doi.org/10.1016/j.engstruct.2020.111243
Received 18 December 2019; Received in revised form 13 August 2020; Accepted 17 August 2020

Training and Research in Earthquake Engineering (EUCENTRE) conducted "Progetto Scuole", a research project aimed at investigating the seismic vulnerability of Italian school buildings. A comprehensive database was developed for approximately 49,000 school buildings in Italy by Borzi et al. [10]. Data related to structural behaviour, as well as other features concerning school organisations, was collected. From the database, it was observed that approximately 80% of school buildings in Italy are made of unreinforced masonry (URM) and reinforced concrete frames with masonry infill (RC), whereas the remaining 20% are characterised by other typologies, such as precast (PC), steel or mixed steel-concrete structures [11,12].

The knowledge of the main features of the existing school building stock allowed the identification of representative case study school buildings in order to perform detailed loss estimation studies and to identify adequate retrofit strategies.

The well-known performance-based earthquake engineering (PBEE) methodology, proposed by Cornell and Krawinkler [3], and subsequently developed by the Pacific Earthquake Engineering Research Center (PEER) in California as the PEER-PBEE methodology, is applied in a systematic fashion in this study to perform the seismic loss assessment [4] of three case study school buildings, representative of different structural typologies, namely RC frames with masonry infill, URM buildings and PC structures. The results of the seismic assessment and loss estimation pointed out the deficiencies of these school buildings, as discussed in detail by O'Reilly et al. [13], and showed that non-structural elements play a key role in the monetary losses. As reported by Taghavi and Miranda [14], the initial monetary investment in non-structural elements for office/schools, hotels, and hospitals buildings can reach up to 60% to 90% of the total building value. Similarly, when retrofitting typical Italian buildings, O'Reilly and Sullivan [15] demonstrated that in situations where collapse performance is not a critical issue, the retrofitting of non-structural elements can have a much larger impact on expected annual loss (EAL) reduction when compared to traditional structural interventions, which in some cases actually worsened the EAL due to excessive floor accelerations caused by strengthening and stiffening.

In this study, the influence of different retrofit techniques, addressing both structural and non-structural elements, on the reduction of EAL and the achievement of code requirements was investigated in order to identify the best retrofit options, as well as to provide useful considerations on the most suitable approaches to be followed for different building typologies. Moreover, the impact of reducing the EAL and the benefit of implementing a retrofit intervention both on structural and non-structural elements, was investigated through a cost-benefit analysis. The PEER-PBEE methodology was applied to characterise the current performance of the case study school buildings using more advanced metrics. Fig. 1 summarises the steps that were followed. The seismic vulnerabilities of the school buildings were also assessed through non-linear static analyses [16] to evaluate the structural performance at different limit states defined by the Italian National Code (NTC 2018) [17] and to apply the seismic classification guidelines recently introduced in Italy [9].

2. Summary of existing case study buildings

The data collected in the EUCENTRE database of school buildings [10], as well as the results of previous studies [18–21], were used to identify the main features of existing school buildings in Italy and the main sources of structural vulnerability. The construction period was found to be a preliminary indicator of the seismic vulnerability [18–21]. Table 1 lists the construction typology, number of storeys and constructions periods of the three case study school buildings extracted from the database and analysed in this study. The selected buildings are relatively regular in both plan and elevation. This building configuration is typical for school buildings, although more irregular buildings from that construction period can be found in Italy. As described by O'Reilly et al. [13], an in-situ building survey was carried out for each building to gather information and create an inventory of damageable structural and non-structural elements. From a structural point of view, all the information required to identify the main deficiencies of the buildings was collected, including also the possible degradation of structural elements and, for the PC case study school building, the details on the beam-column connections and on the connections between the cladding panels and the frame structure.

2.1. Numerical modelling

Based on the in-situ surveys, advanced non-linear numerical models were developed to simulate the structural seismic response of the three case study school buildings. The main features of the numerical models are reported in the next sections; more details can be found in O'Reilly et al. [13].

2.1.1. Reinforced concrete case study school building

The OpenSees software [22] was used to develop a numerical model of the RC case study school building. To account for all possible deficiencies related to RC structures designed before the 1970s in Italy, the modelling recommendations by O'Reilly and Sullivan [23] were followed. Beam and column members were modelled as force-based beam-column elements with a modified Radau plastic hinge integration scheme, as suggested by Scott and Fenves [24] that provides a lumped plasticity component. Frame elements included a post-peak strength and stiffness degradation, while the non-linear behaviour of beam-column joints was simulated using zero-length elements, as illustrated in Fig. 2. The slab was assumed to be rigid based on its structural configuration. The stair cases were modelled using elastic frame elements to consider the potential shear failure of the surrounding columns. The numerical model also included the effect of exterior masonry infill walls. As shown in Fig. 2, masonry infill walls were represented through an equivalent diagonal strut, as proposed by Crisafulli et al. [25].

2.1.2. Precast concrete case study school building

The numerical model of the PC case study school building was also developed in OpenSees [22], as illustrated in Fig. 3. The structural system comprises precast columns that support precast beams in the longitudinal direction. The absence of precast beams in the transverse direction was confirmed from the in-situ survey. The precast columns were modelled with a lumped plasticity approach following Haselton et al. [26] recommendations. Due to the lack of continuity in the beam-column joints, no moment transfer was assumed between adjacent beams. For this reason, the beams were modelled as elastic elements. The slab's bending stiffness was explicitly modelled to account for the lack of structural connections and the absence of beams in the transverse direction. A detailed numerical model was developed to simulate the beam-column connections through rigid elements to represent the depth of the beam and zero-length elements at its top and bottom to simulate a gap effect and contact seat, respectively. The cladding panels were incorporated into the numerical model following the recommendations by Belleri et al. [27].

2.1.3. Masonry case study school building

The URM case study school building was modelled in TreMuri [28], a specialized software suitable for the seismic analysis of 3D masonry buildings. The model uses an equivalent frame approach to simulate the behaviour of the building (Fig. 4). This modelling approach takes into account the two main components in a masonry wall: the piers and the spandrels. The piers act as the main vertically resisting elements, while the spandrels couple the response of two adjacent piers. The non-linear macro-element implemented in TreMuri allows two main failure modes to be simulated: 1) flexural failure, expressed as rocking and crushing mechanisms; and 2) diagonal cracking and shear sliding to account for

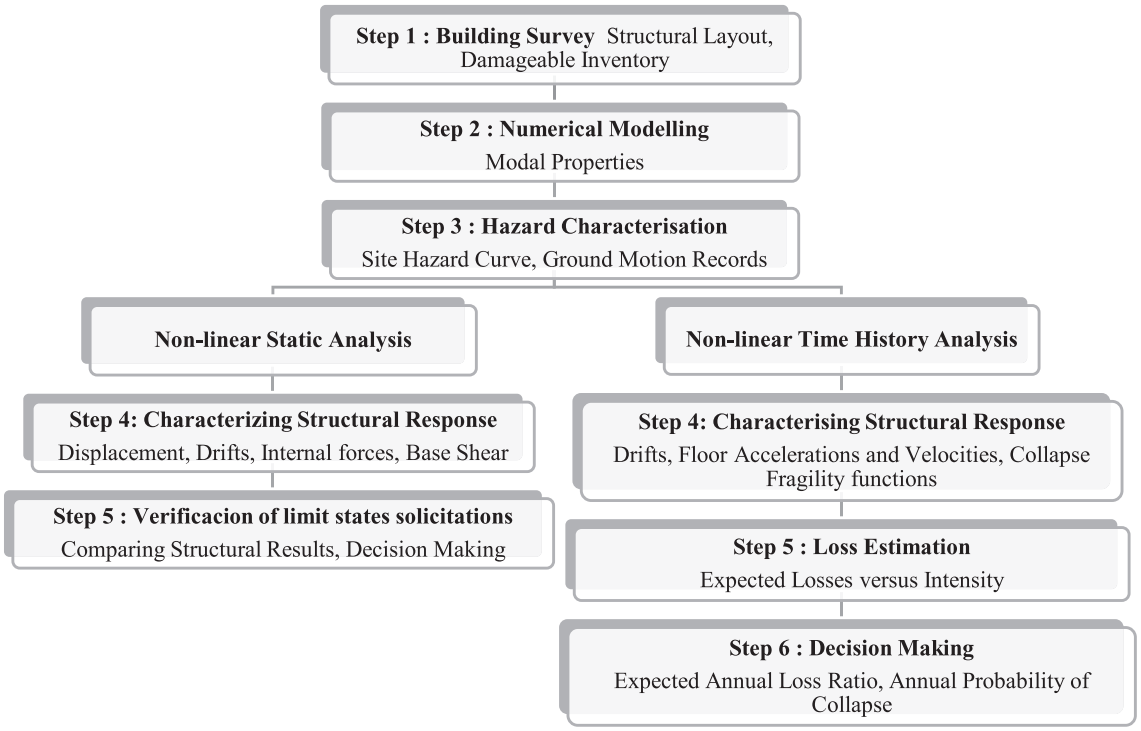

Fig. 1. Steps of the performance assessment, based on the PEER-PBEE methodology [3], applied to the case study school buildings.

shear failure. The failure of the panels is defined in terms of a drift limit. If the maximum storey drift in a pier is achieved, the element becomes a strut, meaning that shear and bending capacity are reduced to zero, while the axial load is still supported. Following NTC 2018 [17], it was considered reasonable to set the drift limit for shear and bending failure at 0.4% and 0.8%, respectively.

Second-order geometrical P-Δ effects were taken into account for all the case study school buildings. The inherent damping in the URM case study school building was defined through a 5% tangent stiffness proportional Rayleigh damping model, whereas constant 5% critical damping to all modes of vibration was assumed for the RC and PC case study school buildings [29]. Cracked section stiffness was assumed in the numerical analyses, as proposed by O'Reilly et al. [30]. Table 2 reports the results of the eigenvalue analyses carried out on the three case study school buildings. The elastic fundamental periods reported in Table 2 were used to characterise, by different conditioning periods, the hazard curves necessary for the analyses, as described in the next section.

2.2. Seismic hazard characterisation

Probabilistic seismic hazard analysis (PSHA) was conducted for the city of Cassino, Italy - the actual location of one of the selected case study school buildings. This site is considered representative of a medium-high seismicity in Italy [31]. Therefore, using the seismic demand of this site served to characterize the vulnerability of the case-study buildings, as well as to compare their seismic response when exposed to the same seismic hazard. This assumption will not foresee significant issues since these building typologies can be found anywhere in Italy [10,13]. Adopting the hazard model proposed by Meletti et al. [32], this location is characterised by a peak ground acceleration (PGA) of 0.21 g for a return period of 475 years. The sets of ground motion records [13] were chosen to match a conditional spectrum generated with the REASSESS software tool [33]. A total of 22 pairs of ground motion records in two horizontal components were taken from the PEER NGA-West 2 database [34]. Furthermore, the spectral acceleration, Sa(T*) at a conditioning period, T*, was chosen as the intensity measure (IM) for the hazard curve. The arithmetic mean of the two computed orthogonal fundamental periods was used to define T*, as suggested in FEMA P58 [4] and reported in Table 2 for each case study school building. The hazard curves for each conditioning period T* are shown in Fig. 5.

Moreover, for the structural performance assessment, the uniform hazard spectra (UHS) were also calculated at different return periods for the selected site. The following four return periods were considered according to the prescriptions provided by NTC 2018 [17]: 45, 75, 712 and 1463 years, corresponding respectively, to SLO: operational limit state, SLD: damage limitation limit state, SLV: life safety limit state and SLC: collapse prevention limit state, for a building class III with a nominal life of 75 years, which would correspond to a school building.

2.3. Structural response

The structural performance of the case study school buildings was assessed through non-linear static and dynamic analyses. Fig. 6 shows the static pushover curves of these buildings, expressed in terms of base

Table 1
General information for case study school buildings, adapted from [13].

Typology	Label	No. of storeys	Construction period
Reinforced concrete frame with masonry infill	RC	3	1960s
Unreinforced masonry	URM	2	1900s
Precast RC frame	PC	2	1980s

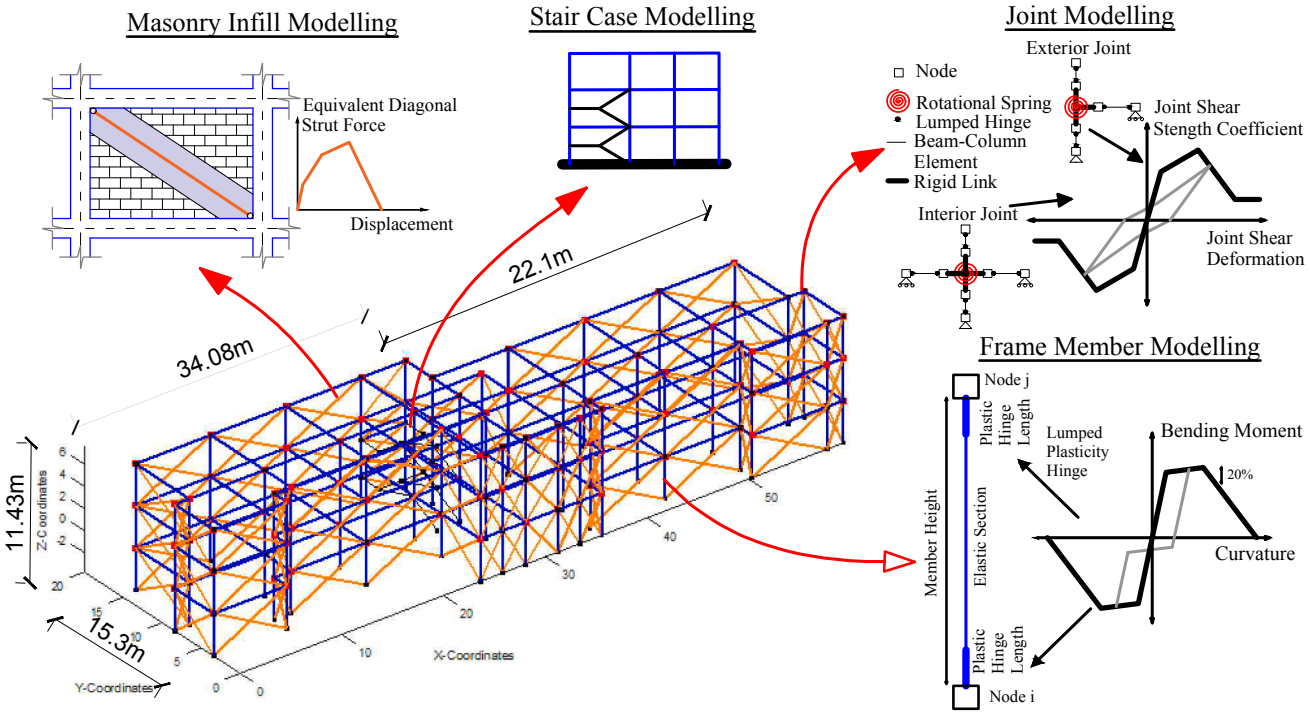

Fig. 2. Main Features of the numerical model of the RC case study school building, adapted from [13].

shear coefficient (ratio between the base shear capacity and seismic weight of the building) and the building roof drift (roof displacement/total building height). The performance points corresponding to the four limit states, also plotted in Fig. 6, were identified according to the following criteria: SLO as two thirds of the suggested drift for limiting the damage to non-structural elements specified in NTC 2018 [17]; SLD as the minimum between the drift at incipient yielding in a structural element and the recommended drift limit [17]; SLV as the drift at maximum lateral capacity; and SLC as the drift after reaching a drop of 20% of SLV lateral capacity.

The SLD drift limits are described as 0.5% for a building with rigid partitions (adopted for the RC and PC school buildings), and 0.2% for unreinforced-masonry structures (adopted for the URM school building). Due to the type of failure mechanism observed in the URM case study school building, the SLV and SLC limit states for this typology were assumed to be achieved when the building reached a drift

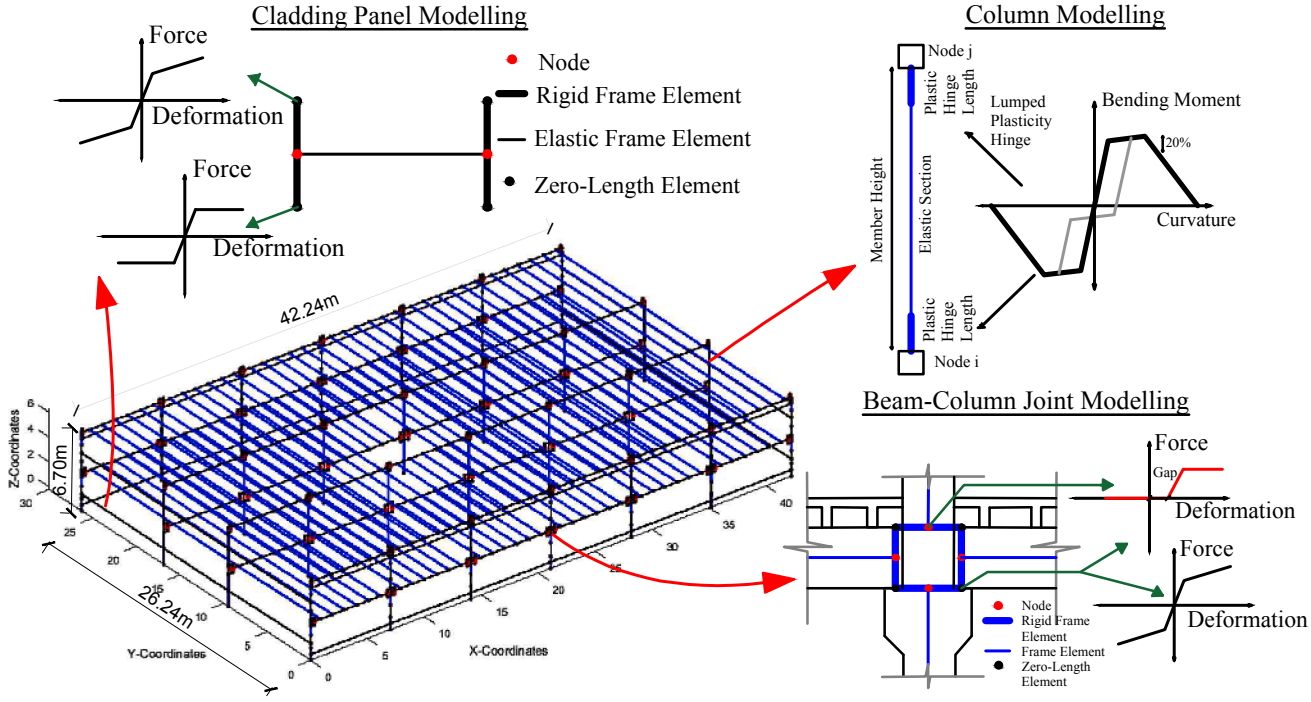

Fig. 3. Main features of the numerical model of the PC case study school building, adapted from [13].

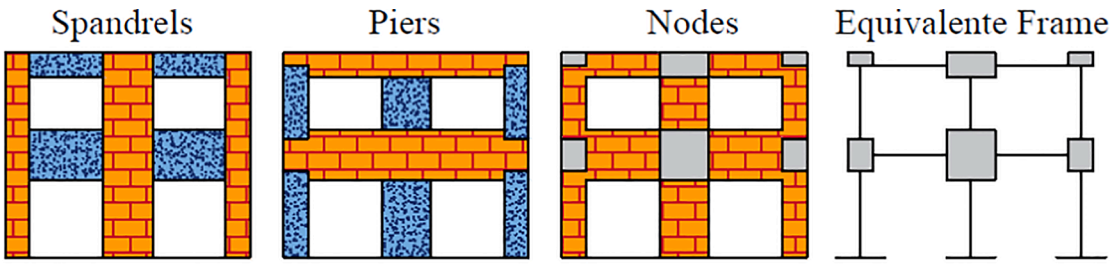

(a) Equivalent in-plane frame idealisation of the URM walls using TreMuri [28].

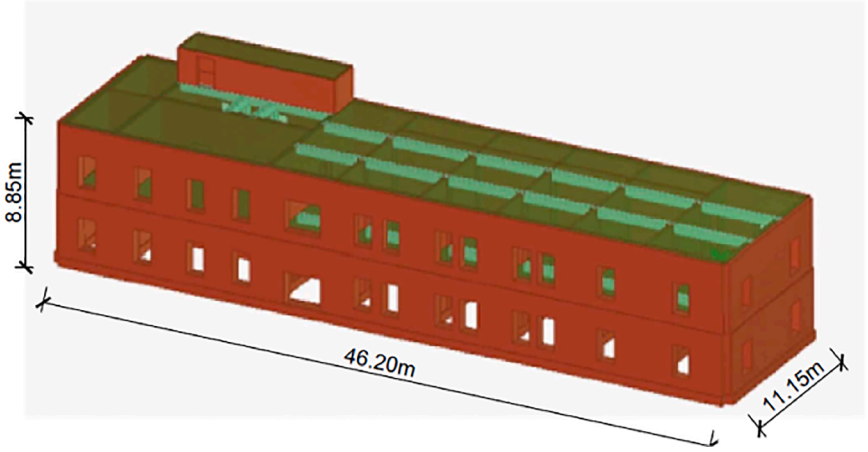

(b) 3D view of URM case study school building.

Fig. 4. Main features of the numerical model of the URM case study school building, adapted from [13].

of 0.4% and 0.6%, respectively. These values, suggested by Morandi et al. [35], are conservative for describing the incremental damage undergone by URM structures when shear is the dominant failure mode. For the bare RC building, the SLV and SLC limit states were determined based on the capacity of the bare RC frame structure, following the recommendations established by NTC 2018 [17] and Eurocode [36]. The lateral capacity of this assembly in both directions is significantly different if the masonry infills are considered or not (i.e. BARE in Fig. 6a), while for the PC case study school building the lateral capacities in the two directions are similar. The PC case study school building shows the highest displacement capacity, while the URM case study school building is characterised by the lowest lateral strength and deformation capacities.

In order to evaluate the structural performance of the case study school buildings, the N2 method [17] was implemented, considering the structural requirements of NTC 2018 [17]. For the RC configuration, the approach outlined by Dolšek and Fajfar [37,38] was used since it deals with the performance of RC frames with infill walls. The serviceability limit states (SLO and SLD) were assessed according to the drift limits proposed by NTC 2018; this verification is illustrated in Fig. 7a. On the other hand, the requirements for the ultimate limit states (SLV and SLC) imply maintaining the vertical stability and the development of a ductile mechanism, which avoids soft-storey or weak-storey failure and promotes the strength hierarchy criteria presented by Tasligedik et al. [39].

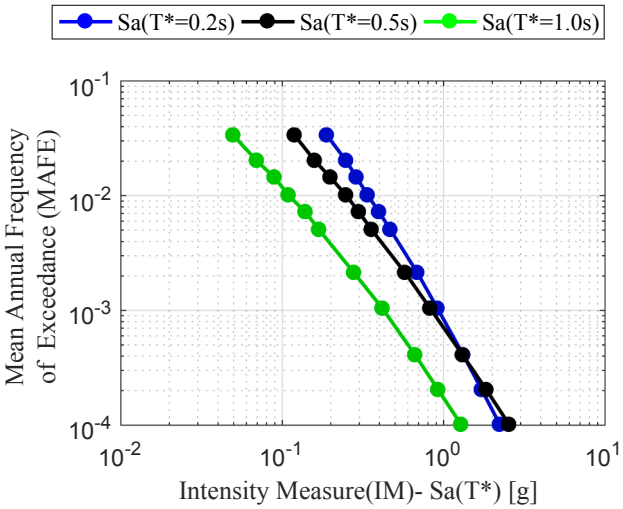

Fig. 5. Hazard curves at conditioning periods T* for Cassino, Italy.

Fig. 7 illustrates the distributions of maximum storey drifts along the building height for each return period considered. The RC case study school building is the only structure meeting the drift criteria at the serviceability limit states, while the PC and URM case study school buildings largely exceed the drift limits, being more detrimental in the

Table 2
Translational elastic mode periods of the numerical models and adopted conditioning periods.

School building	Longitudinal mode period ($T_{1,X}$)	Transverse mode period ($T_{1,Y}$)	Arithmetic mean period ($T_{average}$)	Conditioning period (T*)
RC	0.36 s	0.61 s	0.49 s	0.50 s
PC	1.10 s	1.11 s	1.11 s	1.00 s
URM	0.22 s	0.49 s	0.36 s	0.20 s

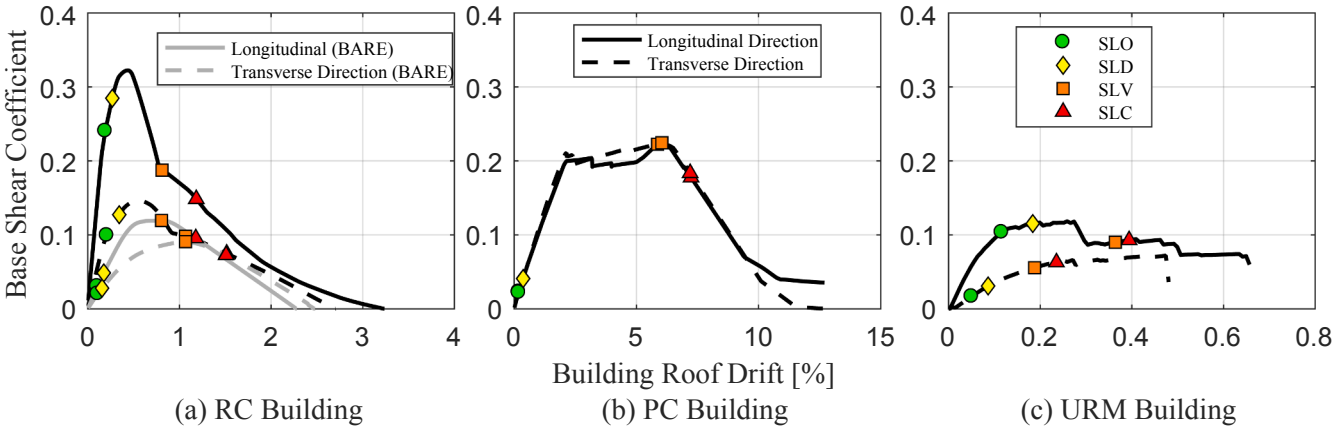

Fig. 6. Static pushover curves for the case-study school buildings in both orthogonal directions, where the base shear is normalised by the total building weight and the point at which each of the limit states are exceeded is marked (NTC – 2018 [17]). (a) Lateral capacity RC building, (b) Lateral capacity PC building, c) Lateral capacity URM building.

case of the PC structure. In terms of the ultimate limit states, the RC and PC case study school buildings exhibit drift concentrations, which can be related to the lack of lateral storey strength and/or stiffness. No results are shown in Fig. 7 for the URM case study school building at these ultimate limit states since its pushover curve does not intersect with the life safety demand intensity, meaning that it is expected that it would have collapsed already. These results highlight the very high seismic vulnerability of this building.

The local response of the structural elements was also investigated to define the best retrofit strategies for the case study school buildings. Fig. 8a presents an illustrative example of the strength hierarchy of a beam-column joint in the RC case study school building. The figures

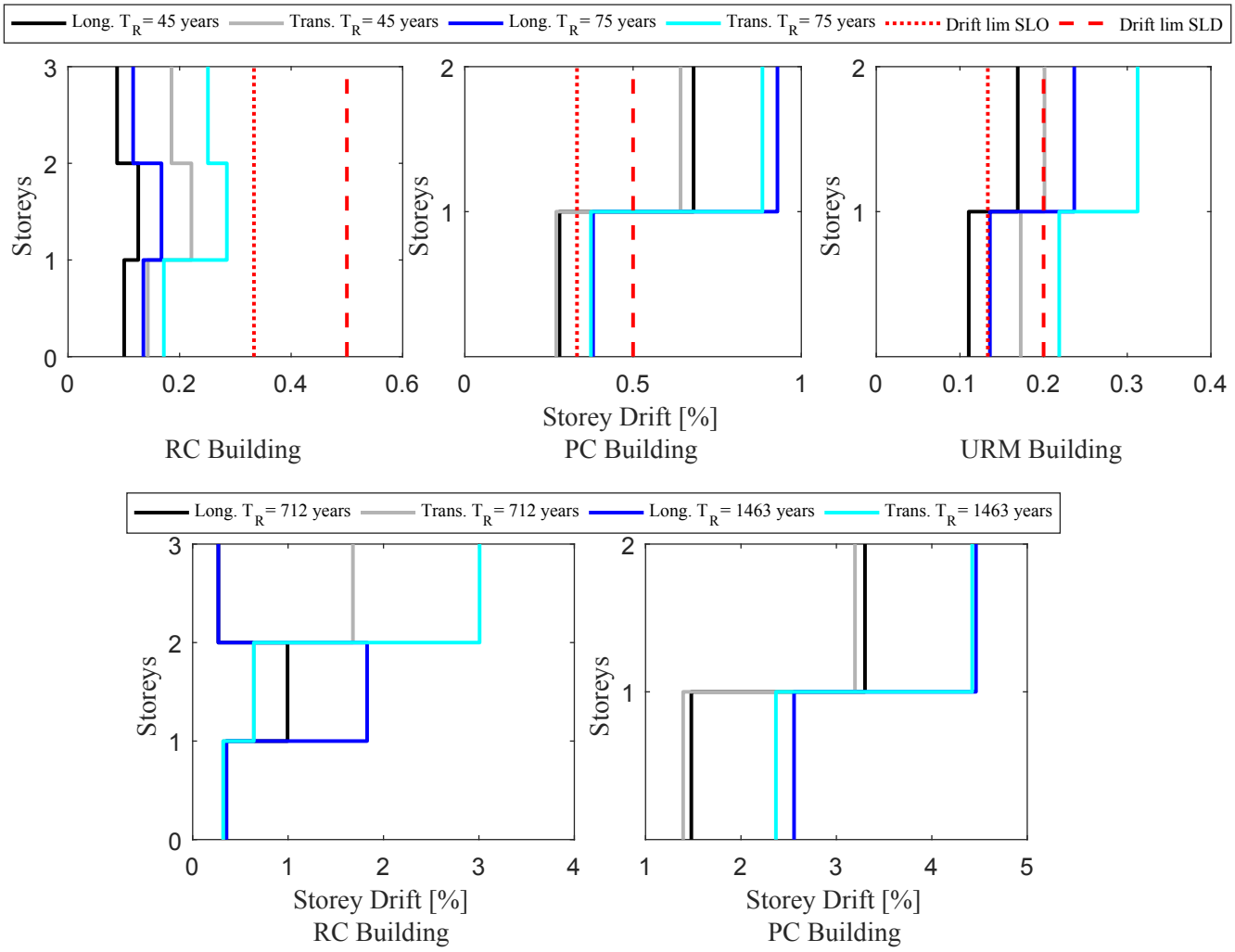

Fig. 7. Maximum storey drifts in case study school buildings at different limits state intensities specified in NTC 2018 [17].

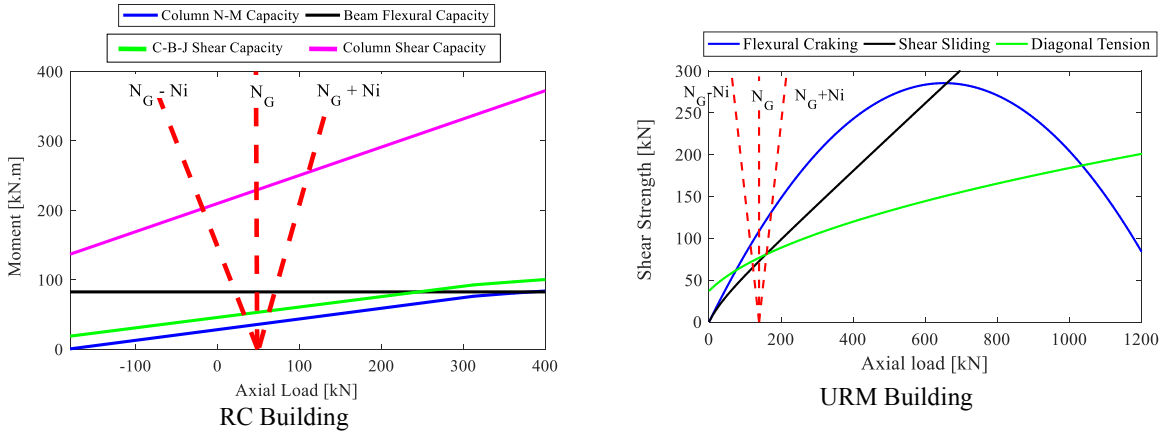

(a) (left) Failure capacity in column-beam joints in RC case study school building and (right) failure capacity of masonry wall piers in URM case study school building.

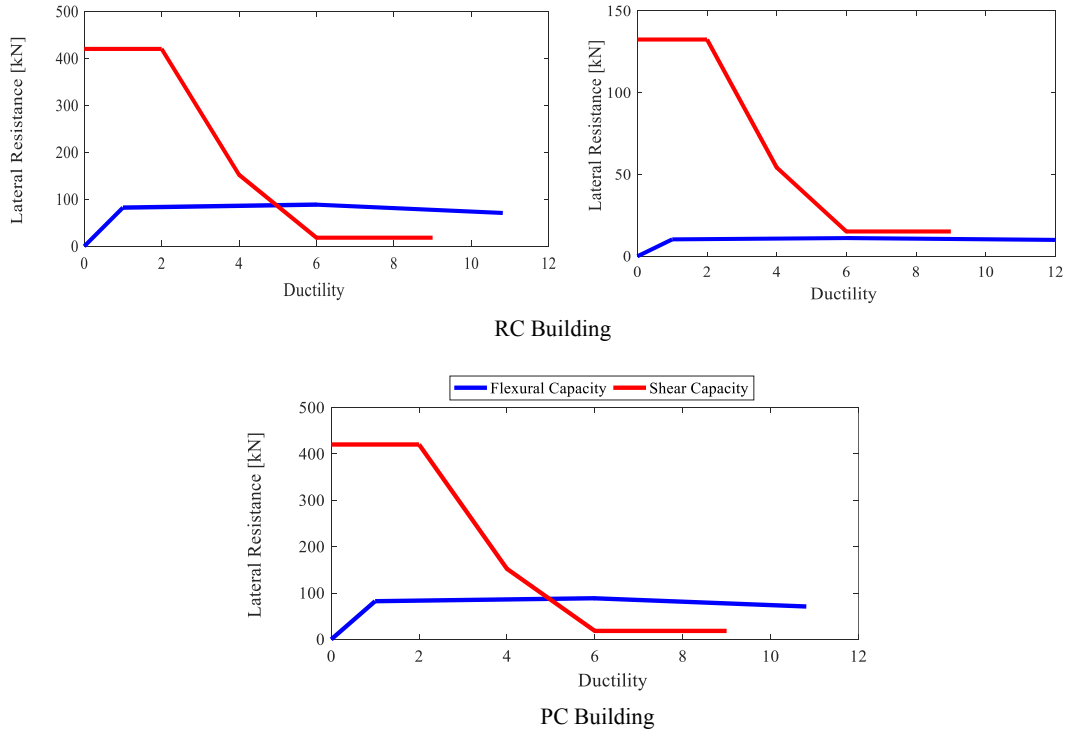

(b) Illustrative example of the flexural capacity and shear capacity of columns as function of their ductility.

Fig. 8. Examples of strength hierarchies in RC and PC case study school buildings.

also show an example of the strength criteria comparison for a pier (macro-element) in the URM case study school building. The strength hierarchy assessment described by Tasligedik et al. [39] was applied to perform the assessment. This method allows the weakest element within a RC column-beam joint to be identified as a function of the flexural capacity and considering the variation of axial load acting within a joint. Several joints in the RC case study school building were found to have an undesirable failure mechanism, which may explain the drift concentrations illustrated in Fig. 7. An example of this behaviour is illustrated in Fig. 8a, where the strengths of a particular column and joint in the RC case study school building are below the strength of the beam for the range of axial loads acting on the joint. This type of failure sequence initiates a column-sway mechanism leading to a non-ductile failure mode. A similar approach was used to evaluate the structural behaviour of the URM case study school building; however, for this case, only the piers were verified since they are the main elements resisting the lateral loads. Three failure modes were considered for the piers: flexural cracking, shear sliding and diagonal tension [28]. Fig. 8a shows that, as for the analysed pier element, the failure mechanism is controlled by the diagonal tension and shear sliding. This undesirable behaviour was observed for most of the piers of the URM case study school building.

Alternatively, the combined flexural and shear capacities of columns as function of their ductility, proposed by Galal and Ghobarah [40], were determined to verify the expected column behaviour. This approach employed the model presented by Priestley et al. [41] to estimate the shear capacity in the columns. Fig. 8b illustrates the combined capacity for the RC and PC case study school buildings. It can be observed that a moderate ductile behaviour (i.e. when the flexural capacity and shear strength intersect for a ductility higher than 4) and ductile (i.e. when these two curves do not intersect), as defined by Galal and Ghobarah [40], is expected for the columns in both buildings.

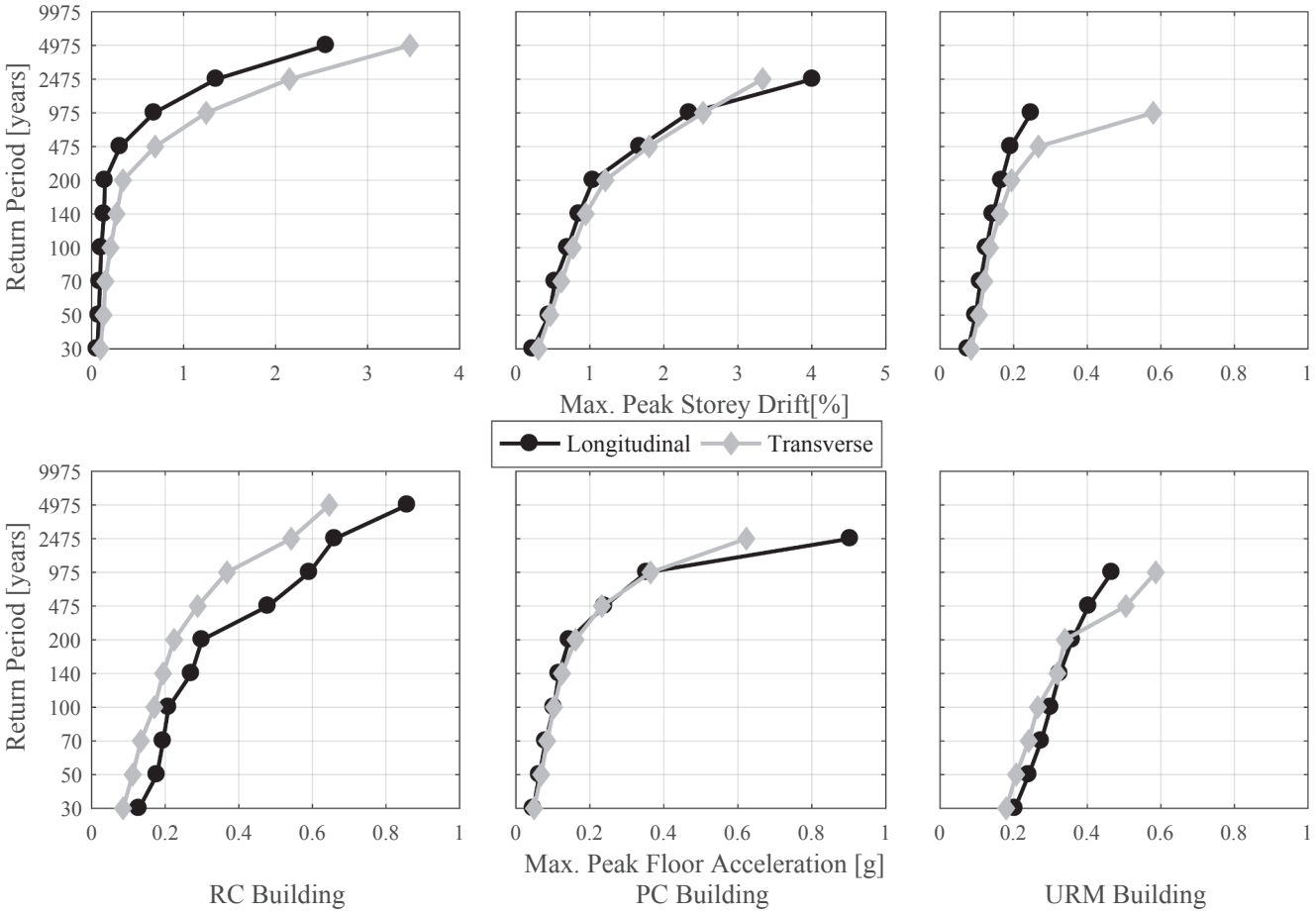

Fig. 9. Median peak storey drifts and peak floor accelerations over the height of the case study school buildings in both principal directions.

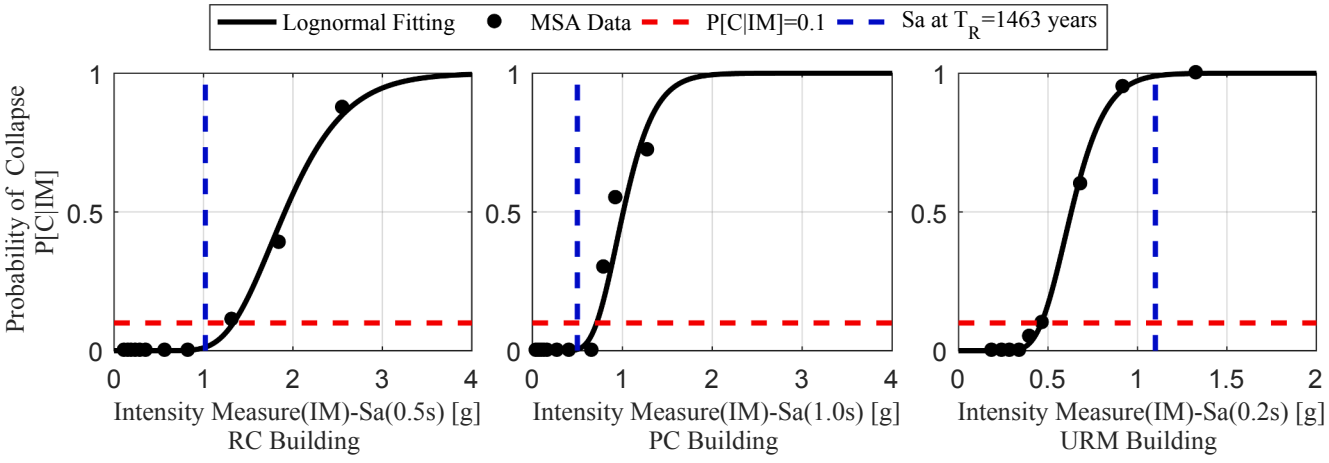

Fig. 10. Collapse fragility functions for the case study school buildings.

Similarly, no brittle failure is expected for the columns of both case study school buildings. As such, special attention has to be paid to the failure sequence shown in Fig. 8a in order to achieve a proper strength hierarchy in the RC and URM case study school buildings. The performance assessment illustrated in Figs. 7 and 8 evaluates the main code requirements [17], demonstrating that in many cases the buildings are not meeting the NTC 2018 requisites for diverse limits states. Consequently, retrofit interventions need to be considered to satisfy the code provisions.

Non-linear response history analyses (NRHA) were then conducted following the multiple-stripe analysis (MSA) methodology, using the ground motion records described in Section 2.2. Fig. 9 illustrates the response of the different case study school buildings in terms of median value of the maximum peak storey drifts (PSD) and peak floor accelerations (PFA), along the building height, in both principal directions. The drift demands for the RC and PC case study school buildings are larger than that of the URM case study school building. This highlights the flexibility of these buildings when compared to the URM structure, which is stiffer. The RC case study school building is both stiffer and stronger than the PC case study school building due to the presence of the masonry infills. This can also be verified through the translational mode periods listed in Table 2 and the drift profiles plotted in Fig. 7.

Table 3
Median collapse intensities, θ, dispersion due to record-to-record variability, β_R, dispersion due to model uncertainty, $\beta_{MU,}$ total dispersion, β_T, median collapse intensity at collapse prevention limit stated, Sa at T_R = 1463 years and collapse margin ration, CMR, for each case study school building.

School building	Median IM, θ	Dispersion, β_R	Dispersion, β_{MU}	Dispersion, β_T	Sa at T_R = 1463 years	Collapse margin ratio (CMR)
RC	1.91 g	0.28	0.15	0.32	1.02	1.87
PC	1.01 g	0.27	0.35	0.44	0.50	2.01
URM	0.63 g	0.24	0.20	0.31	1.10	0.57

The results of the NRHA were used to construct the collapse fragility function for each building, considering uncertainty due to record-to-record variability through the use of ground motion sets and amplifying it to account for modelling uncertainty [42]. The number of collapses at each intensity level was expressed as a fraction of the total number of records and then used to compute the probability of collapse. These collapse probability data points were then fitted with a lognormal distribution through the maximum likelihood method outlined by Baker [43]. This method is described by a median collapse intensity, θ, and a logarithmic standard deviation, β_R associated with the record-to-record variability as presented in Fig. 10. The numerical values for θ and β_R associated with these collapse fragility functions are listed in Table 3 along with the collapse margin ratios (CMRs), defined as the ratio between the median collapse intensity and the intensity at the collapse prevention limit state (spectral intensity at T_R = 1463 years listed in Table 3). These results along with other sources of uncertainties (β_{MU} and β_T) will be discussed in the next section. For the RC case study school building, collapse was assumed to have occurred when the storey drift exceeded 5% at any level of the building in either direction, according to O'Reilly et al. [44]. Similar considerations on the drift limit to be assumed for the definition of the collapse were pointed out by ASCE 41-17 [45] and Rossetto and Elnashai [46]. The same drift limit was assumed to define the probability of collapse for the PC case study school building, considering that reaching 5% drift involves excessive columns' plastic hinge rotations and unseating of the beams from the column corbels. For the URM case study school building, collapse was evaluated in terms of failure of the pier elements due to shear or flexure mechanisms. The maximum drift limit assumed for reaching collapse was taken as 0.5%, as defined [23] in the NTC 2018 [17] as the shear failure mechanism for pier members at the ultimate limit state; this value is also suggested by Rota et al. [47].

2.4. Loss estimation and collapse performance

A loss estimation assessment was carried out for each case-study school building. The total expected losses at different intensity levels E[LT|IM] were determined according to Eq. (1), in which P[C|IM] represents the probability of collapse for a given intensity level IM, determined from Fig. 10. The labels C and NC in Eq. (1) denote the collapse and no collapse cases, respectively and RepC represents the total replacement cost of the building.

$$E[LT|IM] = E[LT|NC, IM](1 - P[C|IM]) + P[C|IM]\cdot RepC \quad (1)$$

The epistemic uncertainty, β_{MU}, was introduced in the assessment to consider the modelling uncertainties, whereas the aleatory uncertainty, β_R, was associated with the record-to-record variability. These values are presented in Table 3. The epistemic uncertainty was adopted from FEMA P58 guidelines [4] according to each building typology. The total dispersion β_T was obtained as the square root sum of the squares (SRSS) of β_{MU} and β_R. For the RC case study school building, empirical values proposed by O'Reilly and Sullivan [48] for the epistemic uncertainty were adopted to account for the increased dispersion in the PSD and PFA demands. For the URM and PC case study school buildings, the corresponding values were adopted from the FEMA P58 guidelines [4]. Additionally, residual drifts were also considered for each case study school building. The loss calculation was performed in the software PACT [49] for 11 return periods resulting in 200 realisations. Fig. 11a illustrates the vulnerability curve describing the loss ratio associated with each return period. The expected losses reach the replacement cost at a different return period for each case study school building. For the URM case study school building, the expected losses equal the replacement cost (i.e. expected loss ratio = 1) near the 475-year return period. For the RC and PC case study school buildings, the expected loss ratio reaches a value equal to unity near the 2475-year return period.

The collapse performance of each case study school building was assessed according to the FEMA P695 methodology by verifying that the probability of collapse under maximum considerable earthquake (MCE) ground motions (P[C|MCE] is less than 10%. The return period associated with the MCE intensity level was defined according to NTC 2018 and is equal to 1463 years. The CMR values, presented in Table 3, are very similar for the RC and PC case study school buildings (approximately 2.0) meaning that these buildings present a considerable safety margin against collapse. On the other hand, the CMR for the URM case study school building is lower than unity, highlighting once again the building's vulnerability to collapse (i.e. P[C|MCE] > 50%). Another approach to assess the collapse performance is to integrate the collapse fragility curve over the entire hazard curve to obtain the mean annual frequency of collapse (MAFC), which is presented in Fig. 11b for each case-study school building. Dolšek et al. [50] reviewed typical acceptable MAFC limits obtained from various studies available in the literature and noted that this limit is in the range of 10^{-5} to 10^{-4}, which are represented by the red dotted horizontal lines in Fig. 11b. It is clear that the performance of the URM case study school buildings is unacceptable. Furthermore, even if not as prominently, the RC and PC case study school buildings also fail to meet the acceptable MAFC limits as well. Based on these considerations, the seismic performance of the case-study school buildings should be improved through appropriate structural retrofit interventions to meet code requirements and evaluate their influence on the collapse performance. In other words, the effectiveness of the retrofit interventions should also consider their impacts on the EAL, CMR, MAFC and cost benefit analysis.

The obtained EALs, computed using Eq. (2), are listed in Table 4 for each case study school building along with the assumed RepC. The URM case study school building is the most vulnerable in terms of EAL, followed by the RC and PC case study school buildings. The EALs reported in this study are in line with other results available in the literature. For example, Cardone and Perrone [51] examined the performance of an existing RC frame building with masonry infill located in L'Aquila and reported EAL values between 0.75% and 1.07%. Considering that L'Aquila is characterised by a much higher seismicity with respect to the Cassino site considered herein, the findings of Cardone and Perrone [51] are in line with the EAL value reported in this study. A similar range was also highlighted in Perrone et al. [52] for infilled RC frames located Italy. Similarly, Sousa and Monteiro [53] and O'Reilly and Sullivan [14] have analysed pre-1970 RC frames with masonry infills in different Italian locations characterised by low to high seismicity, and obtained EAL ranging from 0.2% to 0.5%; hence, again, in agreement with the results presented here. Ottonelli et al. [54] examined two case study URM buildings located in L'Aquila and reported EAL values between 0.55% and 0.68%, which again align reasonably well with the findings herein, considering the relative differences in seismicity. Lastly, Cornali et al. [55] examined existing PC frame

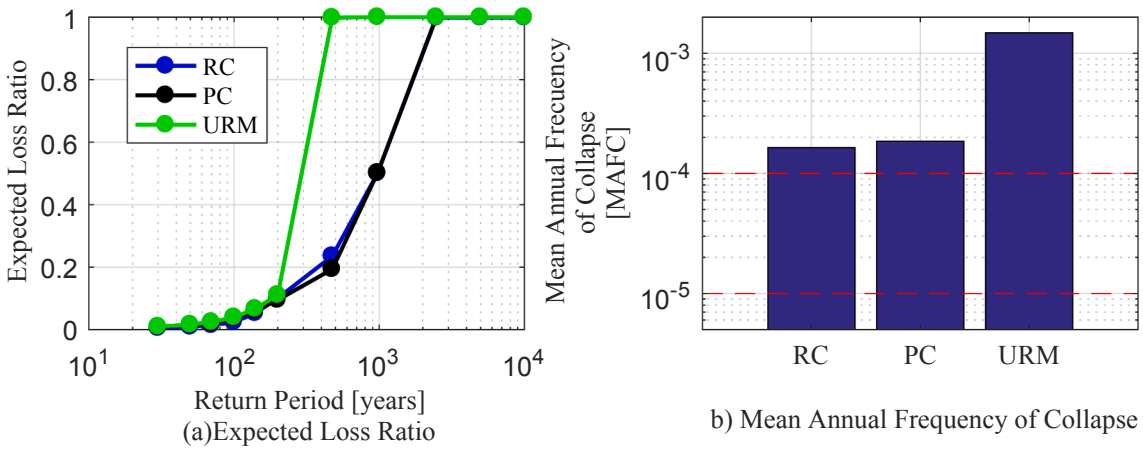

Fig. 11. Loss estimation of case study school buildings, (a) expected annual loss vs return period and (b) mean annual frequency of collapse (range of acceptable MAFC limits according to Dolšek et al. [50] indicated by horizontal dotted red lines). (For interpretation of the references to colour in this figure legend, the reader is referred to the web version of this article.)

Table 4
Expected annual loss ratios, EAL, and total replacement cost, RepC, for each case study school building.

School building	EAL [%]	RepC [€]
RC	0.27	3,929,937
PC	0.27	4,212,616
URM	0.43	2,075,892

buildings in Italy and reported EAL ratio between 0.51% and 0.71%, which again are in line with the results obtained in this study.

$$EAL = \int E[L_T|IM] \left| \frac{d\lambda}{dIM} \right| dIM \quad (2)$$

3. Description of retrofitted case study school buildings

The performance assessment and loss estimation study carried out on the case study school buildings pointed out some structural deficiencies, such as excessive drifts and non-ductile collapse mechanisms. At the same time, the collapse performance characterised via MAFC yielded higher values with respect to acceptable limits proposed in the literature [50]. In this section, some retrofit strategies are considered to meet the NTC 2018 [17] requirements for the diverse limit states. It is also expected that this approach reduces the MAFC and mitigate the structural deficiencies of the three case study school buildings. In the development of the retrofit schemes, it is important to keep in mind that by mitigating some structural problems, others might arise. For example, O'Reilly and Sullivan [15] indicated that strengthening and stiffening the structural system are two practical solutions for enhancing the collapse capacity but also may increase the EAL. The benefits obtained through strengthening and stiffening to reduce drift-sensitive losses can be counteracted by higher floor acceleration demands, thereby increasing losses in acceleration-sensitive non-structural elements and subsequently resulting in a net increase in the EAL.

As stated in Section 1, some steps need to be undertaken for determining the most suitable retrofit strategy for each case study school building. Vona and Masi [56] recommended a standard procedure for selecting and designing retrofit configurations. These steps start by defining the seismic demand for the retrofitted building, generally using the same intensity/demand as for new buildings. Then, a structural analysis is performed, evaluating the demand/capacity for each structural element in terms of internal forces. Next, a retrofit intervention for each element whose demand is greater than the capacity is developed. Lastly, the structure is reanalysed, verifying that all the structural elements present a capacity higher that the demand.

According to Holmes [57], the definition of an efficient retrofit solution should start by improving the seismic capacity of vertical elements. This is efficient since it leads to improvement to both the seismic force-resisting system and gravity load-resisting system. The lack of lateral support triggers unacceptable forces or deformation demands on these vertical elements causing excessive lateral deformations. This deficiency can also be addressed by improving connections by means of local retrofit.

Furthermore, in order to reduce the EAL, proper consideration should be given to the retrofit of non-structural elements. FEMA E-74 [58] represents one of the most comprehensive guidelines suppling mitigation details to improve the seismic performance of non-structural elements. Based on the typology of each non-structural element contained in the building, the guideline provides simple measures for their retrofit, based on a combination of prescriptive, engineering required and non-engineered seismic protection measurements. Likewise, NIST GCR 17-917-44 [59] provides detailed approaches on the performance-based seismic design and assessment of non-structural elements.

3.1. Retrofit of the RC case study school building

Two retrofit alternatives were investigated to upgrade the seismic performance of the RC case study school building. The first alternative (Alternative 1) consisted in strengthening structural elements with fibre reinforced polymers (FRP). The use of this technique has been extensively investigated experimentally both for RC and URM structures [60,61]. Its application is fast and relatively simple with low invasiveness that reduces labour cost and time. Additionally, as a lightweight material, FRP does not modify neither cross sectional properties of elements nor overall structural stiffness, as explained by Elnashai and Pinho [62]. Furthermore, FRP is less vulnerable to corrosion in comparison with other materials and its very high tensile strength provides not only strength improvement, but also a better deformation capacity to structural members. The FRP reinforcement was designed to guarantee a ductile failure mechanism in the RC structure, achieved by modelling increased flexural and shear capacity in columns and joints, as illustrated in Fig. 12a. To design and estimate the capacity of external and corner joints, the approach presented by Del Vecchio et al. [63] was employed, whereas internal joints were designed through the procedure outlined by Akguzel and Pampanin [64]. The procedure to compute the new capacity of the elements strengthened with FRP is described in Eurocode [36]. In order to optimise flexural strengthening, a high tensile strength and low modulus of elasticity was sought. With this in mind, unidirectional carbon fibre reinforced polymers (CFRP)

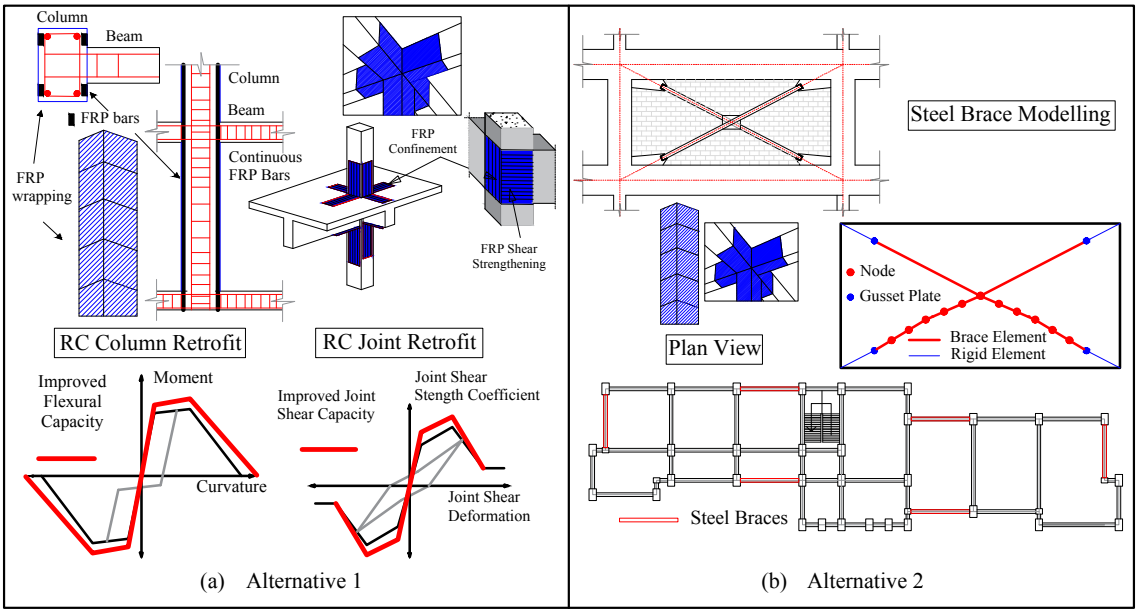

Fig. 12. Illustration of retrofit alternatives for the RC case study school building where (a) Alternative 1 consists of FRP bars, wrapping of columns and FRP strips in joints and (b) Alternative 2 integrates Alternative 1 with steel braces, placed in second and third storeys.

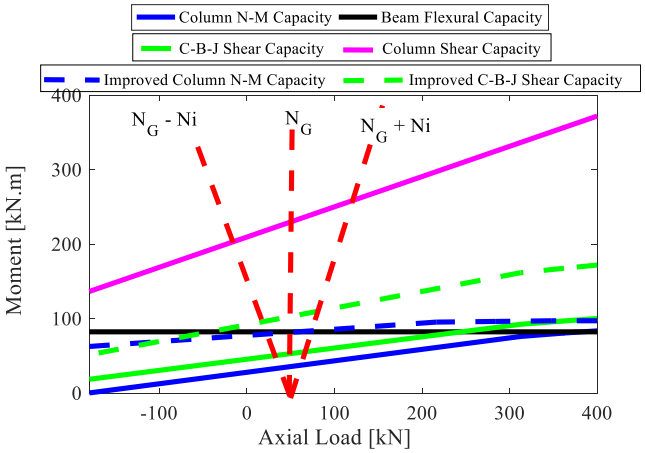

Fig. 13. Strength hierarchy improvement of RC beam-column joints in the RC case study school building.

were adopted. In the case of the columns, two types of CFRP products were assumed: bars and wrapping sheets. Bars were aimed at increasing columns flexural capacity whereas wrapping sheets were targeted to increase their confinement, shear capacity and deformation capacity. Continuous CFRP strips were used for beam-column joints. These strips were placed horizontally and vertically to compensate for the lack of shear capacity. An ultimate tensile strain of 1.6% and elastic modulus of 215 GPa were adopted for the CFRP strips and bars, while sheets were characterised by a low ultimate tensile strain of 0.7%, a high modulus of elasticity of 350 GPa and a tensile strength of 2450 MPa [65]. Additionally, to reduce stress concentration in the FRP due to sharp corners, it was recommended to round the corners with 15–20 mm radii [65]. The increased capacity of the columns and joints, as well as the retrofit interventions, are shown in Fig. 12a. The failure sequence after retrofit is illustrated in Fig. 13, which was employed to size and design the quantity of FRP in each element in other to modify the strength hierarchy. The effectiveness of the FRP in improving the strength hierarchy in a beam-column joint is observed when comparing the strength hierarchy of the original RC configuration (Fig. 8a) with that of the FRP retrofitted building (Fig. 13). On one hand, Fig. 8a shows that the flexural capacities of the joints and columns are weaker than that of the beams whereas the beams in Fig. 13 account for the elements with the weakest flexural capacity, thereby ensuring a ductile failure mechanism.

Even though the first retrofit alternative deals with structural strength deficiencies, it does not reduce the excessive drifts. To deal with this issue, FRP elements were combined with steel braces in a second retrofit alternative. Steel braces can be considered as an efficient solution for the seismic upgrading of RC frame structures. In fact, as stated by Kadid and Yahiaoui [66], steel bracing can work either for rehabilitation of structures damaged by earthquakes or for strengthening of an undamaged building. In the same way, Massumi and Tasnimi [67] illustrated that adding cross bracing to a RC frame of low ductility significantly increases the frame stiffness and modifies its seismic behaviour. This technique is simple, economical, and efficient for strengthening RC frames against seismic forces. The additional stiffness reduces storey drifts and increases the capacity of the seismic force-resisting system, which may prevent a potential soft-storey mechanism. Likewise, considering the ease of construction and the relatively low cost, steel bracing appears to be attractive, when compared to other conventional upgrading techniques, such as adding concrete or masonry shear walls, or even base isolation systems. The retrofit scheme associated with this second alternative (Alternative 2) is illustrated in Fig. 12b, in which braces were introduced in the second and third storeys of the RC case study school building and were connected at their centres to reduce the unbraced length and improve post-buckling resistance. The design of the braces was conducted through an equivalent single-degree-of-freedom system, as described by Di Cesare and Ponzo [68].

To verify the effectiveness of the design assumptions and to define structural details to avoid buckling, a detailed numerical model was developed for the steel braces. In particular, the effect of global buckling in the steel braces was modelled using the recommendations by Lignos et al. [69]. An initial camber proportional to the unbraced length is required to induce in- and out-of-plane buckling, reproducing a realistic behaviour under earthquakes loads. Following the procedure described by Uriz and Mahin [70], it was found adequate to induce a camber of 0.75% for in-plane buckling, while 0.05% was sufficient for out-of-the plane. Likewise, the braces were modelled including rigid elements to account for the geometry of the connections, which connect

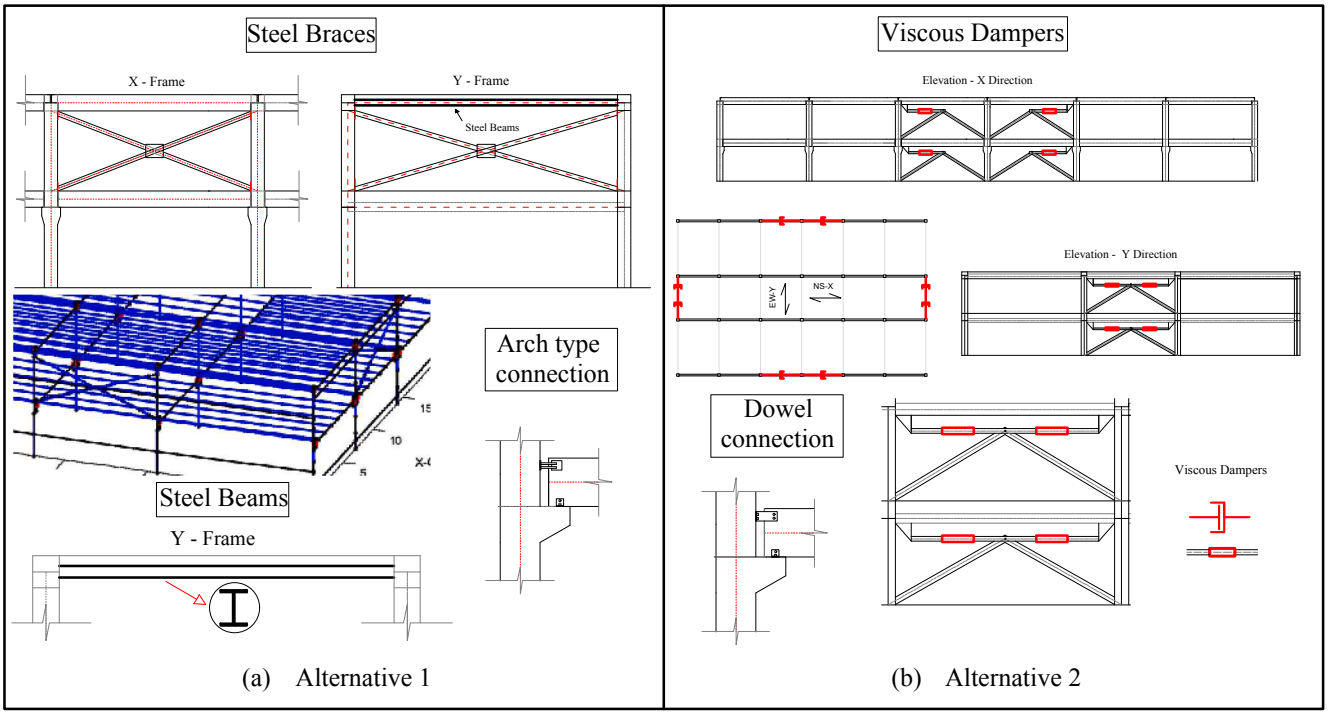

Fig. 14. Illustration of retrofit alternatives for the PC case study school building where (a) Alternative 1 incorporates steel braces and improved connections in the beam-column joints and (b) Alternative 2 incorporates viscous dampers and improved connections in the beam-column joints.

braces, columns and gusset plates to consider the out-of-plane failure. The rigid elements were modelled in OpenSees as elasticBeamColumn elements, the gusset plates as zero-length spring elements and the braces as forceBeamColumn elements. The Giuffré-Menegotto-Pinto material model with isotropic strain hardening was adopted [71]. Each brace was discretised with six elements subdivided into three integration points to consider the effects of nonlinearity. The out-of-plane rotation of the gusset plates was modelled through a pin connection, with a relatively low out-of-plane rotational stiffness.

3.2. Retrofit of the PC case study school building

The vulnerability analysis on the PC case study school building uncovered the lack of continuity in the beam-column joint connections and high storey drift demands. Therefore, two retrofit solutions were studied. The first retrofit alternative (Alternative 1) consisted of implementing arch shape ductile connections in the upper part of the beam-column joints, as shown in Fig. 14a. This type of connection was suggested by Belleri et al. [72] and is composed of double curved circular steel rods welded to rectangular plates anchored to the structural elements. As stated by Belleri et al. [72], the different stiffness and both in-plane and out-of-plane strength properties accommodate the relative displacements between the adjacent connected elements as well as limit the column top displacements, as shown in Fig. 15a. This advantage makes this connection quite effective in controlling displacements and dissipating energy. The behaviour of the lower part of the joint was improved by adding some dowels that are connected with a small steel plate, as illustrated in Fig. 14a. In this way, the horizontal connection capacity between the beam and the column does not depend only on the friction between these two elements but also on the shear capacity of the dowels. The dowel action was estimated from Fib, bulletin 43 [73] using a predicted relationship between the shear force acting on the dowel and the shear slip of the dowel connection. This type of intervention has been proposed for PC industrial buildings since their main cause of damage and/or collapse is related to the lack of continuity and failure of connections, as observed in the 2012 Emilia Romagna earthquake in Northern Italy [74]. This strategy has demonstrated a substantially improved seismic behaviour of PC industrial buildings [74] therefore, is believed to also serve as an attractive retrofit option in PC school buildings. In addition to the new connections type, steel beams were added in the transverse direction to induce a frame behaviour. As a result, continuity and lateral resistance can also be provided in this direction. The methodology proposed by Di Cesare and Ponzo [68] was adopted for the design. The beams were modelled using forceBeamColumn elements considering uniaxialMaterial Steel02 available in OpenSees and accounting for fatigue effects. Steel braces were placed in the second storey to mitigate the soft-storey mechanisms observed in that storey, as confirmed by the storey drift profile shown in Fig. 7. In this way, a more uniform drift profile is achieved with no excessive drifts on the ground floor. As verified in Section 4, the introduction of steel braces in the second storey did not create a soft storey mechanism in the ground floor.

The second retrofit alternative (Alternative 2) considered improving the seismic response of the beam-column joints by introducing dowels in the upper and lower part of the joints, similar to the first retrofit alternative. It also included the presence of steel beams in the transverse direction to guarantee a frame behaviour. The difference of this second retrofit alternative with respect to the first alternative lies in the introduction of linear viscous dampers placed in different locations in the building, as shown in Fig. 14b. Assuming an inherent damping of 5%, it was determined that a supplemental damping ratio of 15% of critical in the first mode of the building would considerably reduce the seismic demand, accounting for a total damping of 20% of critical in the PC case study school building. The amount of supplemental damping was determined by estimating the viscous damper's constant as a function of a storey lateral stiffness distribution of the unbraced structure for the first two fundamental shape modes [68,75].

Other types of dissipaters are available; for example, metallic and friction dampers, which are displacement-activated, need to exceed a threshold displacement before they start dissipating energy. As a result, the dynamic properties of a buildings are altered. The increase of lateral stiffness due to the implementation of such dampers reduces the

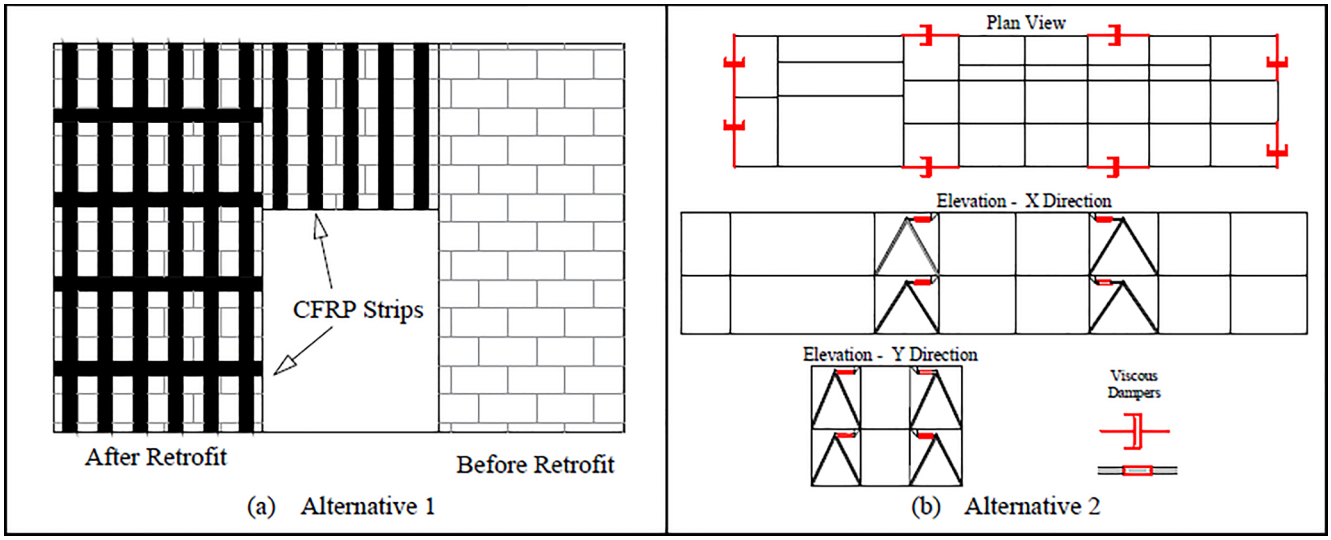

Fig. 15. Illustration of retrofit alternatives for the URM case study school building where (a) Alternative 1 consists of adding FRP strips and (b) Alternative 2 integrates Alternative 1 with viscous dampers.

building's fundamental period [76]. A hysteretic damper retrofit alternative was initially considered but was deemed impractical due to the building's configuration [77]. On the other hand, viscous dampers do not modify the dynamic properties of a building since they are velocity-activated [76]. Therefore, viscous dampers were selected as the most practical solution for energy dissipation and seismic demand reduction for this school building.

3.3. Retrofit of the URM case study school building

It was found that the URM school building did not meet the drift requirements for the serviceability limit states. Additionally, its lateral strength and deformation capacity were not sufficient to withstand the seismic demand at the ultimate limit states, and the structure significantly exceeded the MAFC thresholds. With this in mind, retrofit strategies were devised to increase the structural capacity and to reduce the seismic demand. The results of the as-built vulnerability assessment pointed out the shear failure of the piers (Fig. 8a). To face this issue, the first retrofit alternative (Alternative 1) incorporated CFRP strips on both sides of the masonry piers and spandrels. The design of the CFRP was based on a strength criterion comparison. The strength of masonry elements retrofitted with CFRP was determined by following the procedure described in CNR-DT 200 R1/2013 [78]. Fig. 15a shows the proposed CFRP configuration layout. This retrofit intervention led to a new failure mode as illustrated in Fig. 16, where the shear capacity is increased (dotted lines) and the flexural cracking (blue line) is now the governing failure mechanism. As a result, new drift capacities at shear and rupture for buckling failure were adopted. These values are suggested in TreMuri [28] as 0.6% and 1.2% respectively, which are based on a drift range defined by CNR-DT 200 R1/2013 [78].

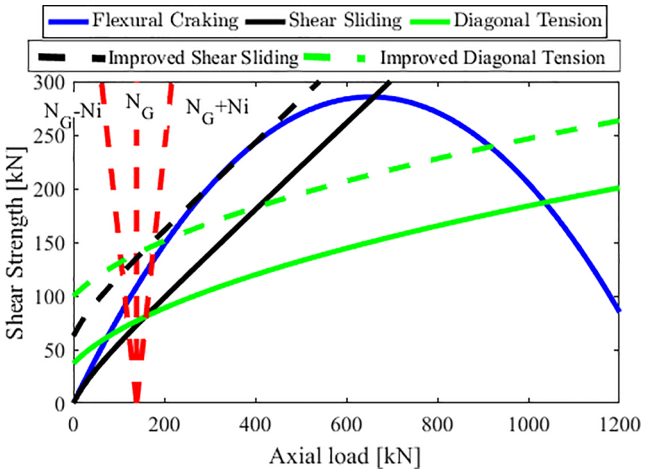

Fig. 16. Improvement of strength comparison criteria for a masonry wall.

A second retrofit alternative (Alternative 2) was also proposed, in which the CFRP strips were combined with the addition of linear viscous dampers placed strategically in the masonry case study school building, as illustrated in Fig. 15b. A total of 16 viscous dampers, eight per floor and four per each principal direction, were included. Assuming an inherent viscous damping ratio of 5% of critical, it was found that a supplemental damping of 35% of critical in the first mode of vibration was needed in the transverse direction (Y) whereas, in the longitudinal direction (X), only 10% supplemental damping was needed. These percentages account for a total of 40% and 15% damping in each principal direction, respectively. Using the option to incorporate the FRP action on the masonry elements featured in TreMuri [28], the amount and properties of FRP strips were defined and assigned in the TreMuri software as a special type of reinforcement. In the case of viscous dampers, their effect was assumed by modifying the Rayleigh damping coefficients according to their participating modes.

4. Assessment of retrofitted case study school buildings

In order to verify the suitability of the proposed retrofit interventions, the performance of the three case study school buildings was re-evaluated using the same approaches previously outlined in Section 2. Particular attention was paid to the overall structural performance, the probability of collapse and the EAL. Finally, a cost-benefit analysis was conducted to gauge the economic feasibility of each intervention.

4.1. Structural performance

Fig. 17 compares the pushover curves before and after the retrofit of the three case study school buildings. All the retrofit alternatives increase the structural capacity of the buildings. For each pushover curve, the capacity points related to each limit state, as described in Section 2.3, were identified.

The effect of the two selected retrofit alternatives for the RC case study school building can be observed in Fig. 17a. The introduction of FRP (Alternative 1) increases both the lateral strength and deformation

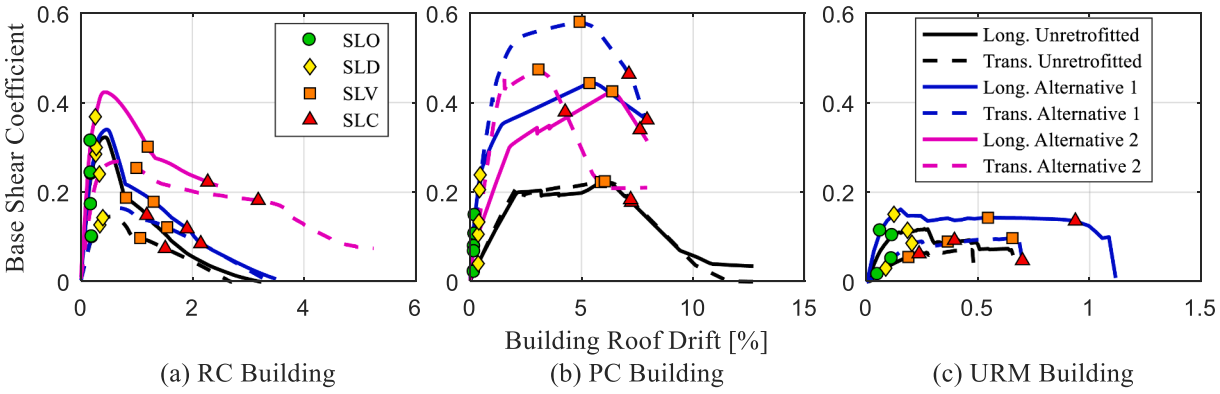

Fig. 17. Static pushover curves for retrofitted case study school buildings, where the base shear has been normalised by the total building weight and where the points at which each of the limit states are exceeded are identified.

capacity in each direction. Alternative 2, which combines FRP with steel braces, significantly increases the lateral capacity in both directions compared to using only FRP. The steel braces also mitigate the soft-storey mechanism in the RC school building. The benefit of FRP for increasing the lateral strength in RC buildings is inhibited by the infills walls. Under the presence of strong infills, horizontal forces are concentrated and transferred directly to the surrounding frame, which does not allow the columns to develop the additional flexural capacity provided by the FRP. Therefore, as described by Gaetani d'Aragona et al. [79], this shear interaction reduces the improvement that FRP can provide.

For the PC case study school building, introducing better connections between precast elements (beams and columns) considerably increased the overall strength of the building. Fig. 17b shows how Alternative 1 rises significantly the stiffness of the system by adding the steel braces. Likewise, the steel beams in the transverse direction contribute to a frame action that greatly improves the structural behaviour and resistance. Alternative 2 demonstrates that the building capacity and its overall behaviour can be remarkably enhanced by providing continuity in the connections through steel dowels. The lateral capacity is derived from the strength of structural elements and connections while the viscous dampers supply supplemental damping to the system, thereby reducing the seismic demand in terms of storey drifts and floor accelerations.

For the retrofit Alternative 1 of the URM case study school building, FRP was adopted as means of increasing the building strength. This retrofit strategy is effective in increasing not only the lateral deformability of the building but also its capacity, as illustrated in Fig. 17c. The higher deformability is reached due to the updated drift shear and bending failure of the FRP material defined as 0.6% and 1.2%, respectively [28,36,80]. In terms of static response, as illustrated in Fig. 17c, Alternatives 1 and 2 overlap, given that the effect of introducing viscous dampers does not affect the lateral static capacity of the building.

The structural performance of the case study school buildings was verified through non-linear static analysis (N2 method), as described in Section 2.3, using the improved pushover curves of Fig. 17. Fig. 18a presents the maximum storey drifts related to the serviceability limit state (SLO and SLD), while Fig. 18b shows the maximum storey drifts for the ultimate limit states (SLV and SLC). Even though the RC case study school building complies with the drift limit requirements for controlling the damage to non-structural elements, both retrofit alternatives modify the response and, in some cases, the drifts are higher but still under the 0.5% limit. Both retrofit strategies for the PC case study school building proved to be effective in reducing the maximum storey drifts, lowering them down to below the limits of 0.5% for SLD and 0.33% for SLO (two-thirds of SLD). In the case of the URM case study school building, both retrofit alternatives decreased the maximum storey drifts. The storey drift profile of Alternative 1 is slightly above the drift limit of 0.2% for SLD, and lower than two-thirds of the 0.2% (0.13%) limit for SLO. However, it can be considered that both retrofit alternatives meet the code requirements related to the serviceability limit states.

Fig. 18b shows that not all retrofit alternatives avoid developing soft/weak storey mechanisms at the ultimate limit state. In the case of the RC case study school building, Alternative 2 works quite well in reducing drifts whereas Alternative 1 is not capable of preventing the soft-storey mechanism from forming. For the PC case study building, both alternatives significantly reduce the drifts. Nevertheless, Alternative 2, which incorporates viscous dampers, achieves a greater reduction and uniform storey drift distribution. This is a result of the supplemental damping that considerably decreases the seismic demand. Finally, for the URM case study building, the ultimate limit state can only be satisfied when adopting Alternative 2. Although Alternative 1 in the URM case study school building increases the building strength and deformation capacity, it is not able to satisfy the seismic demand for the ultimate limit state in the transverse direction. Therefore, no results for this alternative are presented in Fig. 18b.

Moreover, dynamic analyses were carried out in order to evaluate different demand parameters such as peak floor accelerations, probability of collapse and expected losses. Conditioning periods for each retrofit configuration were determined in order to select records to conduct NRHA. Table 5 summarises the dynamic properties of the retrofitted case study school buildings and the considered conditioning periods.

The results of the NRHA are presented in Fig. 20, which shows how Alternative 1 for the RC case study school building practically coincides with the median peak storey drift profile of the original (before retrofit) building. This retrofit alternative increases the deformation capacity of the building since higher intensities are reached. On the other hand, Alternative 2 reduces the median peak storey drifts due to the stiffening action of the steel braces. Similarly, Alternative 1 for the PC case study building decreases the drift profile due to a better connection continuity and stiffer structural system. Likewise, Alternative 2 reduces the peak storey drifts due to the effect of the viscous dampers. It can be observed that drift profiles resulting from both retrofit alternatives are almost identical, suggesting that the action of the steel braces on reducing drifts is similar to the action achieved by the viscous dampers for the amount of supplemental damping considered (15% of critical in each direction). In the case of the URM case study building, both alternatives yield lower peak storey drifts. Alternative 1 slightly increases the stiffness of the system due to the FRP strength improvement, resulting in lower storey drift. Alternative 2 leads to lower seismic demand as a result of incorporating the viscous dampers, thus the drift profile decreases considerably in comparison with the original profile.

The retrofit interventions including steel braces increase the

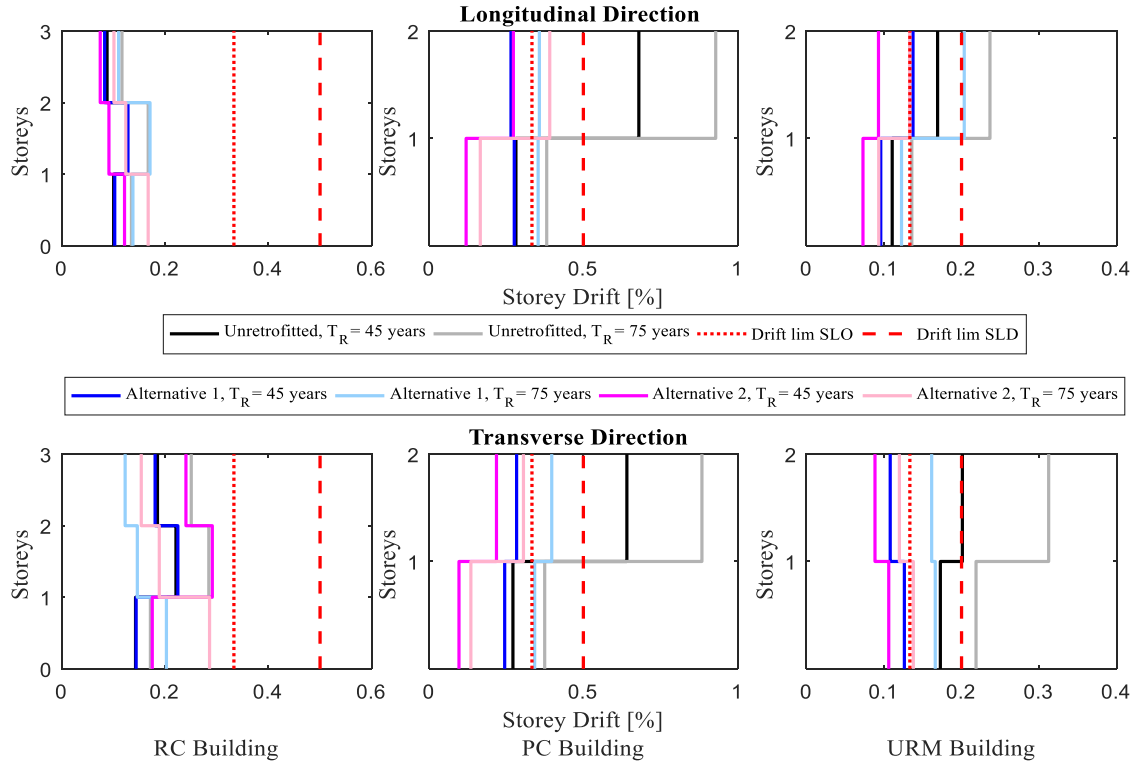

(a) Maximum storeys drifts for the serviceability limit states (SLO, SLD)

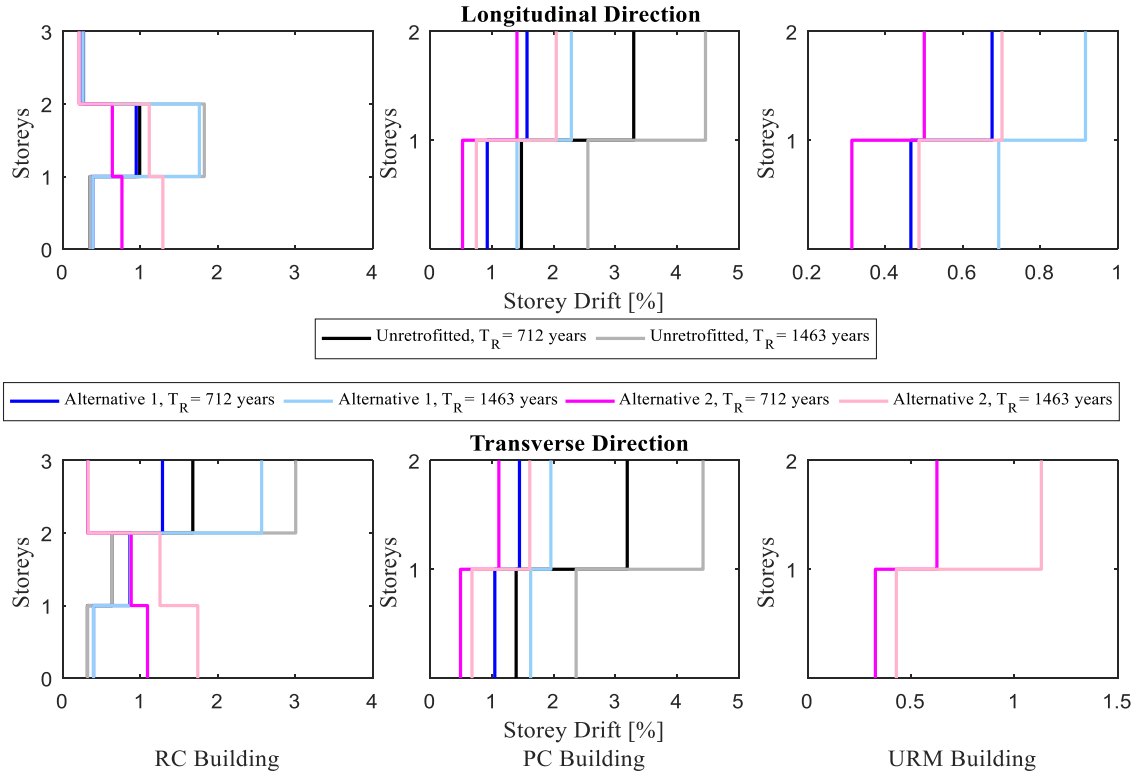

(b) Maximum storeys drifts for the ultimate limit states (SLV, SLC), no drift profiles are shown for the Alternative 1 (FRP) for the URM building in the transverse direction since the demand exceeded the maximum drift capacity.

Fig. 18. Maximum storeys drift at different limits states for the retrofitted case study school buildings.

Table 5
Translational modal periods of the retrofitted numerical models and adopted conditioning periods.

School building	Retrofit Alternative	Longitudinal mode period ($T_{1,X}$)	Transverse mode period ($T_{1,Y}$)	Arithmetic mean ($T_{average}$)	Conditioning period (T*)
RC	Unretrofitted	0.36 s	0.61 s	0.49 s	0.50 s
	Alternative 1	0.36 s	0.61 s	0.49 s	0.50 s
	Alternative 2	0.33 s	0.50 s	0.42 s	0.50 s
PC	Unretrofitted	1.10 s	1.11 s	1.11 s	1.00 s
	Alternative 1	0.46 s	0.58 s	0.52 s	0.50 s
	Alternative 2	0.53 s	0.64 s	0.58 s	0.50 s
URM	Unretrofitted	0.22 s	0.49 s	0.36 s	0.20 s
	Alternative 1	0.20 s	0.44 s	0.32 s	0.20 s
	Alternative 2	0.20 s	0.44 s	0.32 s	0.20 s

structural stiffness of the system and induce higher peak floor accelerations (Fig. 19). This was expected since the fundamental periods have shortened, typically resulting in higher seismic acceleration demand. On the other hand, the introduction of viscous dampers reflects a remarkable reduction of peak floor accelerations, which indicates that the amount of supplemental damping introduced in each building was effective in reducing this demand parameter.

The improved collapse fragility functions achieved by all retrofit configurations are illustrated in Fig. 20. In the case of the RC case study school building, the first retrofit alternative (Alternative 1) proves to be effective in increasing the local element capacity, redistributing the forces and achieving a proper strength hierarchy in the beam-column joints. Consequently, local collapses are delayed since structural elements now require a higher seismic demand intensity to reach local failure. Similarly, the second retrofit alternative (Alternative 2) is less prone to collapse since the combined effect of FRP and steel braces generate a uniform stiffness distribution in each storey and also a higher lateral capacity.

For the PC case study school building, the retrofit alternatives lead to period shortening so that the set of ground motions was conditioned to T* of 0.5 s instead of 1.0 s, which was used for the original (unretrofitted) building. For this reason, no direct comparison can be made between the collapse fragility curves for the retrofitted and the original PC building. However, a general observation indicates that the performance has indeed been improved. The second retrofit alternative (Alternative 2) has a slightly lower collapse vulnerability than that of the first retrofit alternative (Alternative 1). This highlights the importance of achieving a better stiffness distribution and connection continuity rather than adding supplemental damping to the system in order to reduce the collapse vulnerability in a PC structure.

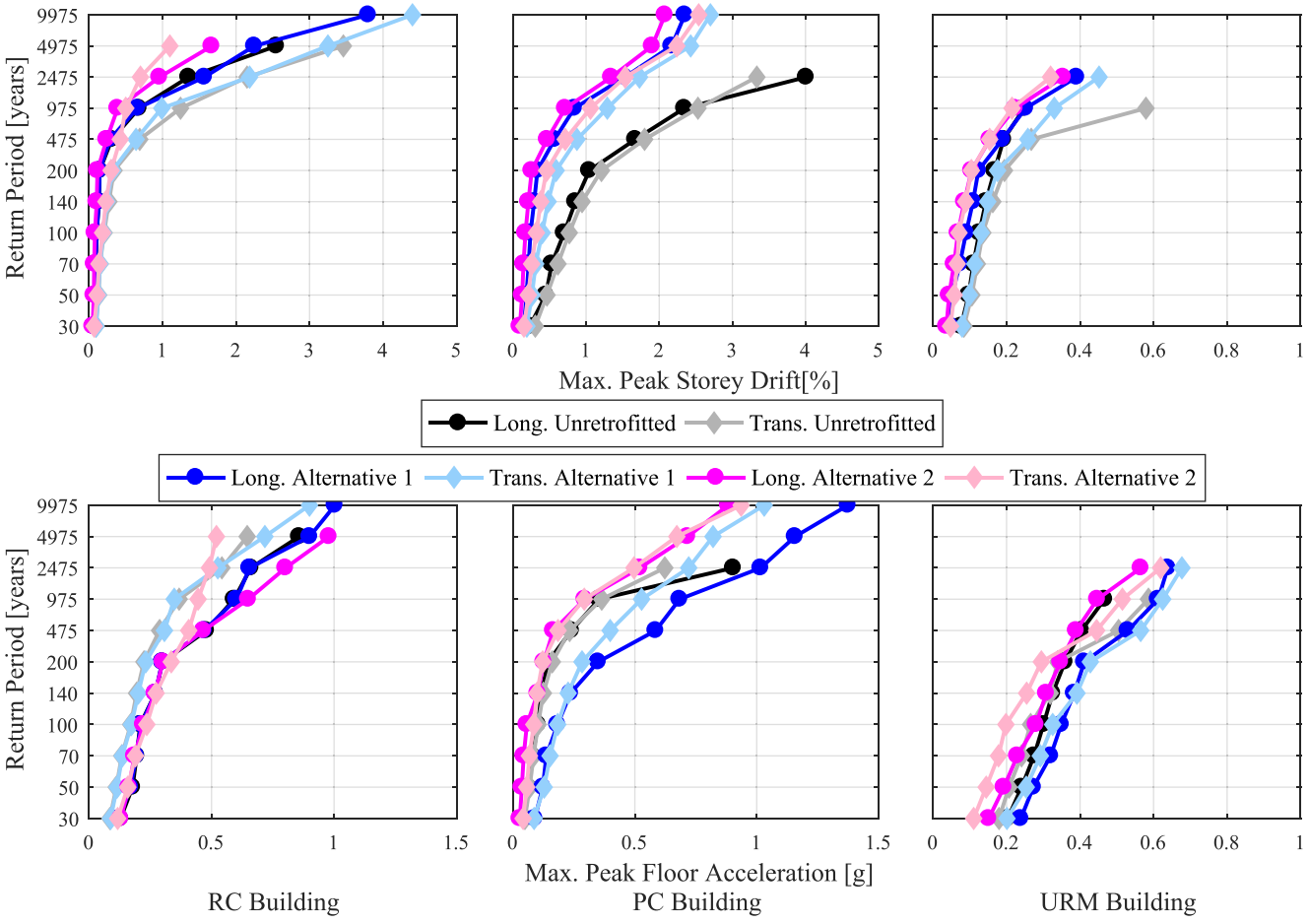

Fig. 19. Median maximum values over the height for peak storey drifts and peak floor accelerations in both longitudinal and transverse directions of the retrofitted and original (unretrofitted) case study school buildings.

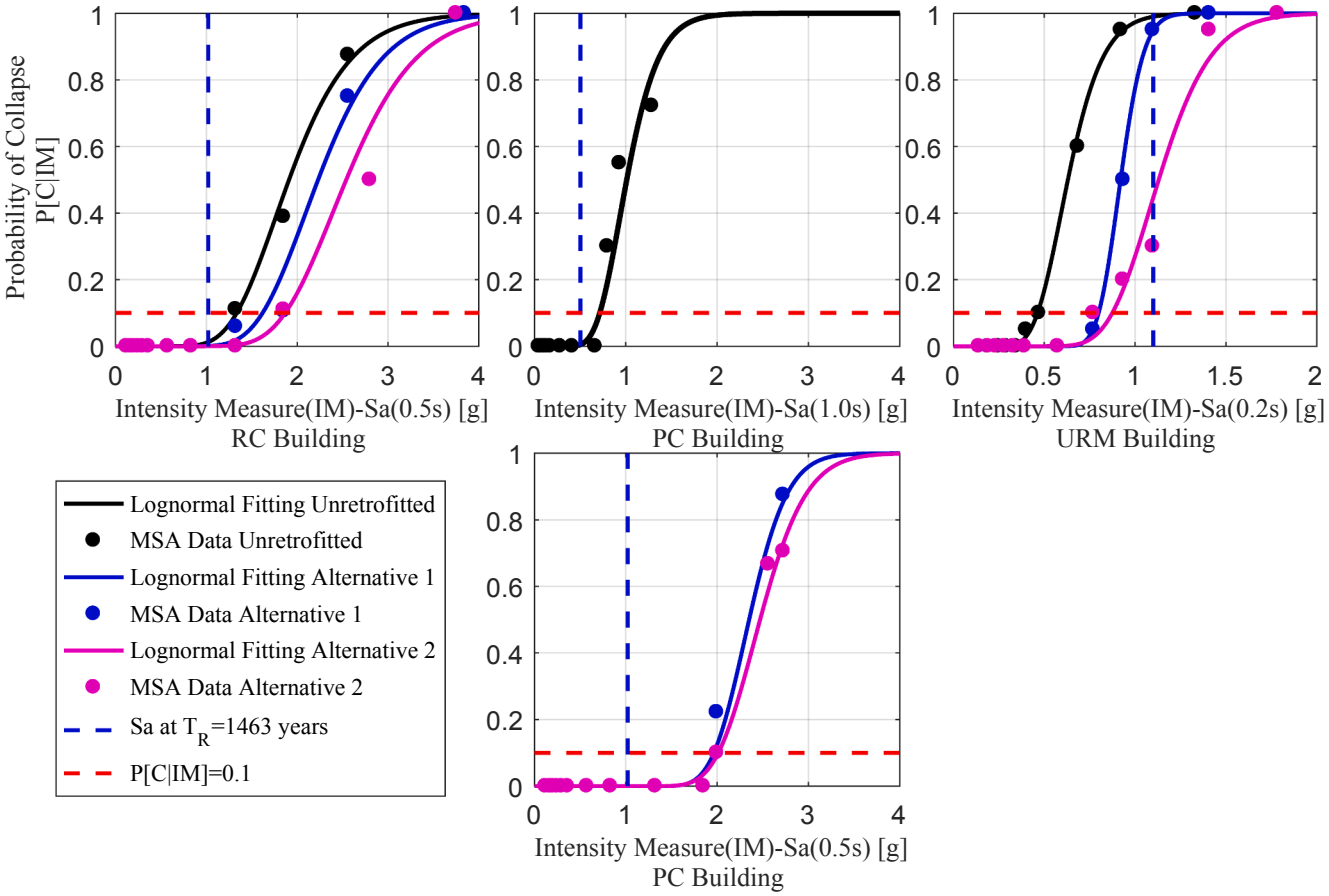

Fig. 20. Collapse fragility functions for retrofitted case study school buildings.

In the case of the URM case study school building, both retrofit alternatives considerably reduce the collapse vulnerability. However, the second retrofit alternatives (Alternative 2) achieves a lower collapse vulnerability.

Another indicator of the improvement of the collapse vulnerability is the collapse margin ratio (CMR), as reported in Table 6. For the RC case study school building, both retrofit alternatives yield a higher CMR compared to the original (unretrofitted) buildings. For the PC case study building, the CMR values for the two retrofitted alternatives demonstrate that they both improve the collapse vulnerability of the building, with the CMR for the second retrofit alternative (Alternative 2) being slightly larger than that of the first retrofit alternative (Alternative 1). Finally, in the case of the URM case study school building, both retrofit alternatives considerably improve the collapse performance of the building. Nevertheless, the first retrofit alternative (Alternative 1), which incorporates FRP, is not sufficient to yield a CMR larger than unity, whilst the second retrofit alternative (Alternative 2) provides a CMR larger than unity, thereby providing the greatest reduction in collapse vulnerability.

4.2. Loss estimation

All retrofit strategies reduce the vulnerability functions of the three case study school buildings, as shown in terms of expected loss ratio in Fig. 21a. In turn, Table 7 lists the numerical EAL values for all retrofit alternatives. Although both retrofit strategies (Alternatives 1 and 2) for the RC case study school building reduce the EAL, this reduction does not seem to be substantial. On the one hand, Alternative 1 presents almost the same acceleration and drift profiles as that of the original (unretrofitted) building thus the EAL tends to be similar. On the other hand, Alternative 2 reduces the peak storey drifts but increases the peak floor accelerations. This likely tends to cause an offset between the expected losses related to drift and acceleration-sensitive elements.

Contrary to the RC case study school building, the second retrofit

Table 6
Median collapse intensities, θ, and dispersion due to record-to-record variability, β_{RTR}, for retrofitted case study school buildings.

School building	Retrofit Alternative	Median collapse intensity, θ	Dispersion, β_R	Sa at T_R = 1463 years	Collapse margin ratio
RC	Unretrofitted	1.91 g	0.28	1.02 g	1.87
	Alternative 1	2.23 g	0.25		2.19
	Alternative 2	2.48 g	0.24		2.43
PC	Unretrofitted	1.01 g	0.27	0.502 g	2.01
	Alternative 1	2.35 g	0.14	1.02 g	2.30
	Alternative 2	2.47 g	0.16		2.42
URM	Unretrofitted	0.63 g	0.24	1.10 g	0.57
	Alternative 1	0.92 g	0.11		0.84
	Alternative 2	1.13 g	0.20		1.03

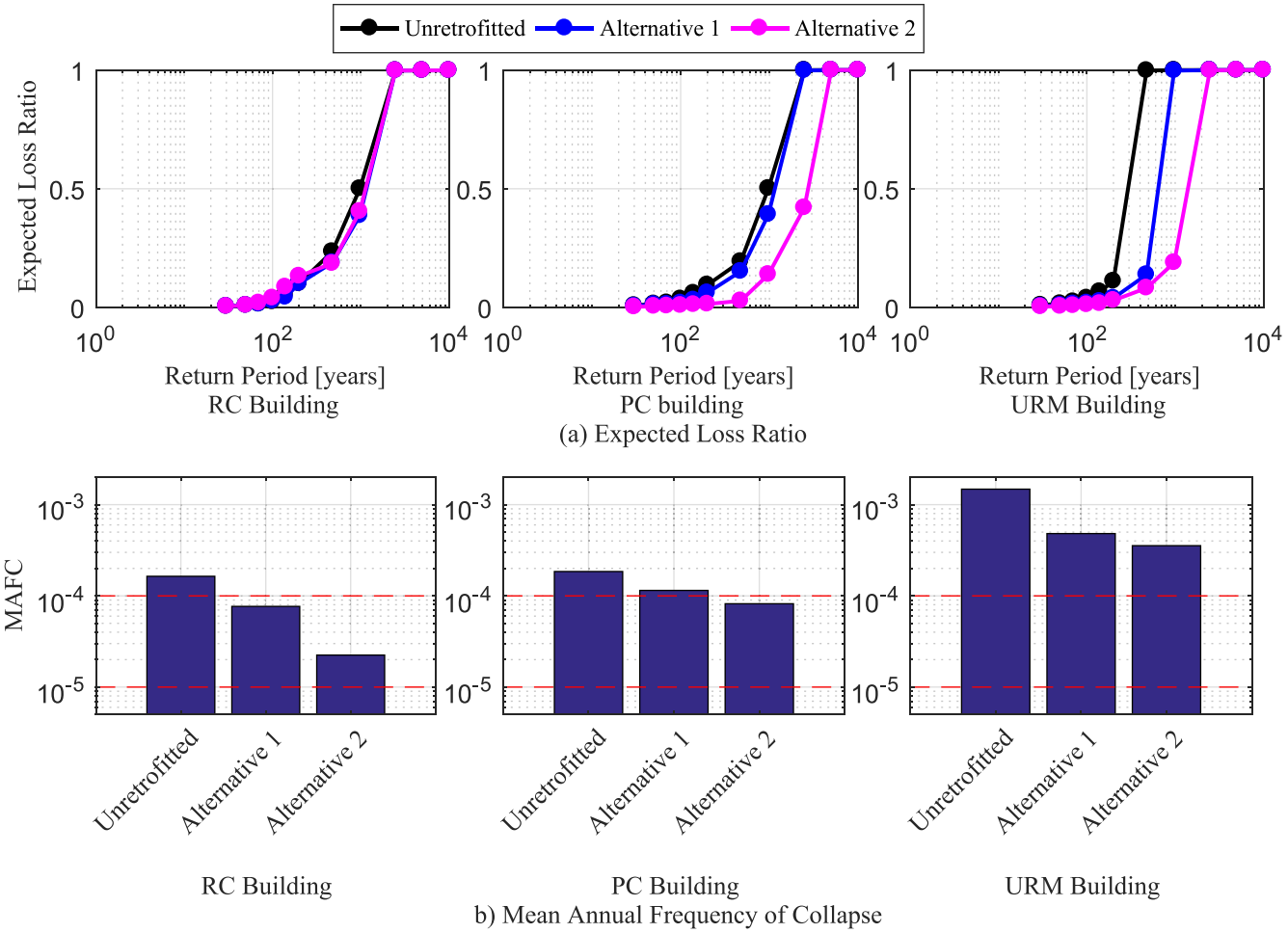

Fig. 21. (a) Seismic vulnerability curves for retrofitted school buildings. (b) Evaluation of collapse performance of retrofitted case study school buildings characterised by the MAFC.

Table 7
Expected annual loss ratio and total replacement cost for retrofitted case study school buildings.

School building	Retrofit Alternative	Expected annual loss [%]	RepC [€]
RC	Unretrofitted	0.27	3,929,937
	Alternative 1	0.25	
	Alternative 2	0.26	
PC	Unretrofitted	0.27	4,212,616
	Alternative 1	0.25	
	Alternative 2	0.09	
URM	Unretrofitted	0.43	2,075,892
	Alternative 1	0.22	
	Alternative 2	0.19	

alternative (Alternative 2) of the PC and URM school buildings achieved a remarkable reduction of the EAL. This is the result of lower peak floor accelerations and peak storey drifts enabled by the viscous dampers. As shown in Table 7, the EAL of each retrofit alternative is based on the total replacement cost of the building. Given that the replacement cost was estimated using a general cost per floor area, rather than an individual component-based cost summation approach, the replacement cost of each building remains unchanged with respect to Table 4. The EAL values obtained with both retrofit alternatives are lower than the values determined for the original (unretrofitted) buildings, further indicating the effectiveness of the retrofit strategies.

In terms of mean annual frequency of collapse (MAFC), both retrofit alternatives of the RC case study school building reduce the risk of collapse, placing the retrofitted building within the acceptable limits suggested by Dolšek *et al.* [50]. For the PC case study school building, the second retrofit alternative (Alternative 2) is the only one achieving a MAFC value within the suggested limits. Despite this, the first retrofit alternative (Alternative 1) achieves a reduction of 38% in MAFC, which is still slightly above the suggested MAFC values. Even though both retrofit alternatives (Alternatives 1 and 2) of the URM case study school building reach a reduction of 67% and 76% in MAFC, respectively, the suggested limits are still largely exceeded.

4.3. Cost-benefit analysis

A cost-benefit evaluation of each retrofit alternative was performed according to a cost-benefit ratio approach, as described in the study by Sousa and Monteiro [53]. This methodology is based on determining the number of years (breakeven point) needed to match the initial cost of retrofit investment during the remaining lifespan of a building, T_{LS} [8]. If the breakeven point exceeds the remaining lifespan of the building, the strategy can be considered of little value from an economic point of view. A lifespan of 100 years (T_{LS}) was considered for the three case study school buildings investigated herein since they are classified as critical facilities [17]. The cost-benefit ratio is calculated according to Eq. (3), in which r is the rate of return that takes into account the change of cash flow over time. $EAL_{unretrofitted}$ accounts for the expected annual loss of the original (unretrofitted) building whereas, $EAL_{retrofitted}$ represents the expected annual loss for the retrofit alternatives. The retrofit costs were estimated based on published

Table 8
Retrofit cost for case study school buildings.

School building	Retrofit Alternative	Cost of Retrofit Intervention [€]
RC	Alternative 1	198,472.75
	Alternative 2	205,690.05
PC	Alternative 1	83,179.27
	Alternative 2	413,474.04
URM	Alternative 1	137,166.57
	Alternative 2	549,104.57

information [80,81] and following recommendations by practitioners and manufacturers. An approximation of the cost for each retrofit configuration is presented in Table 8. The retrofit strategies making use of viscous dampers (Alternatives 2) account for the highest cost and the ones based on FRP (Alternatives 1) for the lowest cost.

$$\mathrm{BCR}(T_{LS}) = \frac{\frac{\sum_{t=1}^{T_{LS}} \mathrm{EAL}_{\mathrm{unretrofitted}} - \sum_{t=1}^{T_{LS}} \mathrm{EAL}_{\mathrm{retrofitted}}}{(1+r)^t}}{\text{Cost of Retrofit}} \quad (3)$$

Different rates of return (r = 0%, 1% and 4%) were considered to evaluate the changes in the trend of the benefit-cost-ratio curve, as illustrated in Fig. 22. The breakeven point, proposed by Cardone et al. [8], is not reached by the retrofit alternatives proposed for the RC case study school building, meaning that in the remaining lifespan of this building it is not possible to fully amortise the cost of the intervention with the benefit achieved by reducing the EAL. In addition, the results are affected by the unchanged EAL obtained for the two retrofit alternatives. The high costs associated with the material and installation of CFRP represent a considerable disadvantage for this retrofit strategy. As observed in Table 8, adding steel braces increases the cost of the retrofit intervention by only €7000 (i.e. from €198,472.75 to €205,690.05), which is a very low amount when compared to the overall cost of Alternative 1. Therefore, the cost of CFRP makes this strategy not economically feasible even though Alternative 2 (i.e. CFRP and steel braces) substantially increases the seismic performance of the school building. For the PC case study school building, the second retrofit alternative (Alternative 2) reaches a breakeven point of 83 years for r = 1% and of 56 years for r = 0%. Therefore, it would be necessary to wait more than half of the lifespan of the building to recover the initial investment of the retrofit interventions. For the URM case study school building, the first retrofit alternative (Alternative 1) achieves a breakeven point of 39 years for r = 1%, and of 32 years for r = 0%. The other retrofit alternatives did not reach a breakeven point for the selected lifespan. In particular, Alternative 2 (i.e. viscous dampers and CFRP) proposed for the URM school building, even though greatly improves the overall performance of the school building, is not an economically feasible strategy, as demonstrated through the cost-benefit analysis. Likewise, an interest rate of r = 4% or higher makes it impossible to reach a breakeven point for any of the retrofit strategies. The decision to retrofit and the choice for a specific retrofit scheme would considerably depend also on other decision variables, such as the priorities of the relevant stakeholders, which would reflect, for instance, on the importance given to the rate of return.

Table 9
Building performance classification ranking as function of both EAL and IS-V prescribed in D.M. 58/2017 [9].

EAL Classification Range	Life Safety Index Classification Range	Classification Ranking
EAL ≤ 0.5%	1.00 ≤ IS-V	A+
0.5% ≤ EAL ≤ 1.0%	0.80 ≤ IS-V ≤ 1.00	A
1.0% ≤ EAL ≤ 1.5%	0.60 ≤ IS-V ≤ 0.80	B
1.5% ≤ EAL ≤ 2.5%	0.45 ≤ IS-V ≤ 0.60	C
2.5% ≤ EAL ≤ 3.5%	0.30 ≤ IS-V ≤ 0.45	D
3.5% ≤ EAL ≤ 4.5%	0.15 ≤ IS-V ≤ 0.30	E
4.5% ≤ EAL ≤ 7.0%	IS-V ≤ 0.15	F
7.0% ≤ EAL		G

4.4. Comparison with the Italian seismic risk classification guidelines

In this section, the seismic risk classification guidelines for Italy described by Cosenza et al. [82] were applied to the three case study school buildings. These guidelines, also known as *Sismabonus*, provide a straightforward risk classification system for existing buildings on the Italian territory. The guidelines are simple to use and can be applied for tax deductions after conducting structural upgrading of buildings. The reduction of taxes is related to the number of upgraded classes achieved by a retrofit intervention. The risk classification is based on two parameters: the life safety index (IS-V) and the EAL. According to the building's performance, both the IS-V and EAL receive a classification ranking, as defined in Table 9. The more critical class between these two parameters defines the overall risk classification of a building. This simple procedure was applied to the case study school buildings as a mean of comparison with the more refined analysis already presented in previous sections.

The IS-V and EAL for each original and retrofitted case study school building were obtained by applying the procedure described in the *Sismabonus* guidelines [82]. The procedure employs the N2 method [16] to find the performance capacity for each limit state (SLO, SLD, SLV and SLC), expressed in terms of PGA. The parameter IS-V is computed as the ratio between the capacity and demand PGAs for the life-safety limit state (SLV), whereas the EAL is estimated through the mean annual frequency of exceedance (MAFE) of the PGA for each limit state. This procedure is comprehensively illustrated in O'Reilly et al. [13] for

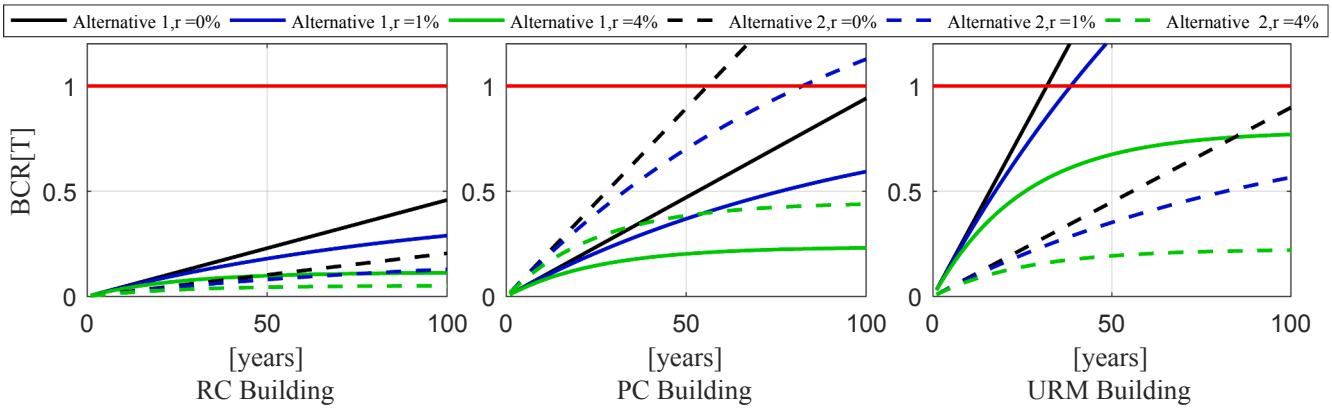

Fig. 22. Cost-benefit analysis for the proposed retrofit alternatives of the case study school buildings.

Table 10
Seismic risk classification for the case study school buildings according to the *Sismabonus* guidelines.

Model	EAL Class	Life Safety Index Class	Overall Classification
RC - Unretrofitted	1.05% - B	0.73 - B	B
RC – Alternative 1	1.44% - B	1.14 - A+	B
RC – Alternative 2	0.76% - A	1.37 - A+	A
PC - Unretrofitted	3.26% - D	2.47 - A+	D
PC – Alternative 1	1.16% - B	4.17 - A+	B
PC – Alternative 2	1.37% - B	2.38 - A+	B
URM - Unretrofitted	2.79% - D	0.45 - C	D
URM – Alternative 1	1.68% - C	0.94 - A	C
URM – Alternative 2	1.46% - B	1.38 - A+	B

the existing case study school buildings considered herein. The risk classification for each original and retrofitted case study school are reported in Table 10.

The results reported in Table 10 are consistent with the outcomes of the refined performance assessment and vulnerability analysis presented in Section 4. The controlling criterion for the risk classification in the RC case study school building and its retrofitted alternatives is dominated by the EAL ranking. In the original (unretrofitted) configuration, the IS-V and EAL yield a class B, which can be considered acceptable according to the ranking classification of Table 9. An improvement is observed with both retrofit alternatives, which upgrade the IS-V index to class A+, but only Alternative 2 (FRP plus steel braces) is able to upgrade also the EAL class, bringing the overall building's class to A. Furthermore for the PC case study school building, the parameter EAL is also the controlling ranking criteria since the IS-V for the original (unretrofitted) and retrofitted PC building configurations (Original, Alternative 1 and 2) is allocated a class A +. Due to the low EAL class for the original (unretrofitted) configuration, the overall class is ranked as D. The two retrofit alternatives upgrade the overall ranking by two classes (B). Lastly, the URM case study school building accounts for the lowest IS-V index, thereby governing for the ranking of the original configuration. The EAL controls the overall ranking in the case of the retrofit strategies. Alternative 2 moves the risk class from class D to class B, while Alternative 1 provided just one class upgrade.

The results of the risk classification documented in this section are logical even though the IS-V and EAL for each building typology and their retrofitted alternatives are different from the values outlined in Section 4. The EAL is overestimated due to the simplification made in the *Sismabonus* methodology, although further refinements have been proposed [e.g. 52]. This risk classification tool is a useful comparison aid, providing a preliminary insight into the overall performance of the building and subsequent retrofit interventions. Additionally, this approach can be practical for building prioritisation. Buildings with low ranking can be programmed for early structural rehabilitation within a risk agenda. Similarly, the most functional retrofit alternative can be selected through the upgrading class achieved by each strategy with respect to the risk classification of the as-built configuration.

5. Conclusions

This paper discussed different retrofit strategies aimed at improving the overall seismic response of school buildings in Italy. These retrofit configurations were examined and evaluated considering the main structural deficiencies. Three case study school buildings were selected and comprised reinforced concrete (RC), precast concrete (PC), and unreinforced masonry (URM) structural typologies. A proper strength hierarchy in beam-column joints was provided for the RC case study school building and a better connection continuity was implemented between the precast elements in the PC case study school building. The structural capacity of the URM case study school building was modified so that flexural cracking in the piers was the controlling failure. The main conclusions arising from this study are summarised as follows:

- The results obtained in this study have highlighted the seismic vulnerability of three existing case study school buildings in Italy, in terms of both economic losses, arising from excessive structural and non-structural damage, and inadequate structural capacity. As expected, the URM case study school building was found to be the most vulnerable building among the three selected buildings. Even though the PC and RC case study school buildings are less vulnerable, they still present structural deficiencies that lead to non-ductile failure mechanisms;
- The effectiveness of fibre reinforced polymers (FRP) in increasing the structural lateral capacity of the RC case study building was limited by the strength of masonry infills. The infills concentrated the horizontal forces and transferred them to the surrounding frame elements, thereby countering the development of the flexural capacity of the columns. Despite this, the deformation capacity was not affected since a higher ductility was developed in the building, thereby reducing the probability of collapse;
- The structural behaviour of the PC case study school building was improved considerably by providing a better continuity in the beam-column joints through dowels and arch-type connections and steel beams placed in the transverse direction, thereby ensuring a better frame action and increased lateral capacity. Despite the high initial retrofit investment, the retrofit alternatives including viscous dampers proved to be more effective in reducing both peak floor accelerations and peak storey drifts, unlike the retrofit strategy incorporating steel braces. Even though this latter retrofit alternative reduced peak storey drifts, the floor accelerations increased due to the increased lateral stiffness provided by the steel braces. This disadvantage offsets the economic losses between drift and acceleration sensitive non-structural elements, yielding a slight reduction in expected annual loss (EAL), when compared to the alternative with viscous dampers;
- Assessing the local failure of the structural elements by means of the strength hierarchy and failure controlling modes prevents undesirable non-simulated failure mechanisms and ensures ductile ones. These criteria were used to design and size the quantity of FRP needed in the RC and URM case study school buildings;
- The rate of return and EAL reduction influence significantly the cost-benefit analysis and thus the overall performance of the retrofitted case study school buildings. Likewise, the cost of retrofit plays a key role, allowing to conclude whether or not a strategy is feasible from an economic point of view. Therefore, the retrofit interventions examined and evaluated for the case study school buildings achieved considerable EAL reductions, considering rates of return lower than 4%;
- The retrofit alternative of the RC case school building that included FRP and steel braces exhibited a better overall performance than that of the retrofit alternative incorporating FRP only. The steel braces mitigated the non-ductile failure mechanisms (soft-storeys), leading to a lower collapse vulnerability and a lower EAL. However, from the economical point of view, neither of these retrofit alternatives were deemed optimal since the initial cost of the retrofit intervention cannot be offset within an expected lifespan of the building. Similarly, the retrofit strategy that incorporated viscous dampers in the PC case study school building resulted in a better overall performance when compared to the retrofit alternative that incorporated steel braces even though both retrofit alternatives enhanced the connections between precast elements and ensured a frame action through the steel beams. Indeed, a breakeven duration of the initial cost of 83 years was reached for a return rate of 1% for the retrofit alternative incorporating viscous dampers. On the other hand, the application of FRP to the URM case study school building improved the failure mechanism in the piers but could not reduce the mean annual frequency of collapse to acceptable limits proposed

in the literature. The retrofit alternative that included viscous dampers in the URM case study school building achieved a greater performance, yet this strategy could not place the building on the safe side, with respect to the mean annual frequency of collapse;

- The new (*Sismabonus)* Italian seismic risk classification guidelines were found to be practical for identifying the relative seismic risk in the case study school buildings, although the computed EAL were in some cases overestimated if compared with more detailed analyses. Nonetheless, the risk classifications were consistent with the findings of the more refined analyses.

CRediT authorship contribution statement

Wilson Carofilis: Conceptualization, Software, Validation, Formal analysis, Resources, Writing - original draft. **Daniele Perrone:** Conceptualization, Resources, Writing - original draft, Writing - review & editing, Supervision. **Gerard J. O'Reilly:** Conceptualization, Methodology, Resources, Writing - review & editing, Supervision. **Ricardo Monteiro:** Conceptualization, Validation, Writing - review & editing, Supervision. **Andre Filiatrault:** Conceptualization, Validation, Writing - review & editing, Supervision.

Declaration of Competing Interest

The authors declare that they have no known competing financial interests or personal relationships that could have appeared to influence the work reported in this paper.

Acknowledgements

The work presented in this paper has been developed within the framework of the project "Dipartimenti di Eccellenza", funded by the Italian Ministry of University and Research at the University School for Advanced Studies IUSS Pavia. The authors express their gratitude to Craig Winters and Bon Schneider of Taylor Devices in North Tonawanda, New York, USA for providing their assistance in estimating the costs associated to viscous dampers as well as to Matteo Moratti of Studio Calvi Srl, Pavia, Italy for his advice on the issues relating to Italian construction practice.

References

[1] Borzi B, Ceresa P, Faravelli M, Fiorini E, Onida M. Seismic risk assessment of Italian school buildings. Computational methods in earthquake engineering. Comput Methods Appl Sci 2013;30(317–344). https://doi.org/10.1007/978-94-007-6573-3_16.
[2] Calvi M, Moratti M, Filiatrault A. Studio della risposta di elementi non strutturali di edifici scolastici soggetti ad eventi sismici/role and importance of non-structural elements in the seismic vulnerability of school buildings (in Italian). Progettazione sismica 2016;6(3):9–29http://dx.medra.org/10.7414/PS.6.3.9-29.
[3] Cornell CA, Krawinkler H. Progress and challenges in seismic performance assessment. PEER Cent News 2000;3:1–2.
[4] FEMA P58-1. Seismic Performance Assessment of Buildings: Volume 1 - Methodology (P-58-1). vol. 1. Washington, DC; 2012.
[5] De Angelis A, Pecce M. Seismic nonstructural vulnerability assessment in school buildings. Nat Hazards 2015;79:1333–58. https://doi.org/10.1007/s11069-015-1907-3.
[6] Grant D, Bommer J, Pinho R, Calvi M, Goretti A, Meroni F. A prioritization scheme for seismic intervention in school buildings in Italy. Earthquake Spectra 2007;23(2):291–314. https://doi.org/10.1193/1.2722784.
[7] Calvi GM. Choices and criteria for seismic strengthening. J Earthquake Eng 2013;17:769–802. https://doi.org/10.1080/13632469.2013.781556.
[8] Cardone D, Gesualdi G, Perrone G. Cost-benefit analysis of alternative retrofit strategies for RC frame buildings. J Earthquake Eng 2017;23:208–41. https://doi.org/10.1080/13632469.2017.1323041.
[9] Decreto Ministeriale. Linee Guida per la classificazione del rischio sismico delle costruzioni - 58/2017, Il ministero delle infrastrutture e dei trasporti, Rome, Italy; 2017.
[10] Borzi B, Ceresa P, Faravelli M, Fiorini E, Onida M. Definition of a prioritization procedure for structural retrofitting of Italian school buildings. COMPDYN 2011-3rd ECOMAS Themat Conf Comput Methods Struct Dyn Earthq Eng, Corfu, Greece; 2011.
[11] Perrone D, O'Reilly GJ, Monteiro R, Filiatrault A. Assessing seismic risk in typical Italian school buildings: from in-situ survey to loss estimation. Int J Disaster Risk Reduct 2019. https://doi.org/10.1016/j.ijdrr.2019.101448.
[12] Terenzi G, Bazzani C, Costoli I, Sorace S, Spinelli P. Advanced seismic retrofit of a mixed R/C-steel structure. Buildings 2019;9:0241.
[13] O'Reilly G, Perrone D, Fox M, Monteiro R, Filiatrault A. Seismic assessment and loss estimation of existing school buildings in Italy. Eng Strt 2018;168:142–62. https://doi.org/10.1016/j.engstruct.2018.04.056.
[14] Taghavi S, Miranda E. Response assessment of nonstructural building elements. PEER report 2003/05, Berkeley, California; 2013.
[15] O'Reilly GJ, Sullivan TJ. Probabilistic seismic assessment and retrofit considerations for Italian RC frame buildings. Bull Earthq Eng 2018;16(3):1447–85. https://doi.org/10.1007/s10518-017-0257-9.
[16] Fajfar P. A nonlinear analysis method for performance based seismic design. Earthquake Spectra 2000;16(3):573–92.
[17] NTC. Norme Tecniche Per Le Costruzioni. Rome, Italy; 2018.
[18] Fiore A, Mezzina M, Porco F, Raffaele D, Uva G. Seismic safety assessment of school building in Puglia (Italy): overview and cases studies. 15th world conference on earthquake engineering. 2012.
[19] O'Reilly G. Performance-based seismic assessment and retrofit of existing RC frame buildings in Italy PhD thesis Italy: IUSS Pavia; 2016.
[20] Buratti N, Minghini F, Ongaretto E, Savoia M, Tullini N. Empirical seismic fragility for the precast RC industrial buildings damaged by the 2012 Emilia (Italy) earthquakes. Earthquake Eng Struct Dyn 2017;46(14):2317–35. https://doi.org/10.1002/eqe.2906.
[21] Penna A, Morandi P, Rota M, Manzini CF, Da Porto F, Magenes G. Performance of masonry buildings during the Emilia 2012 earthquake. Bull Earthq Eng. 2014;12:2255–73. https://doi.org/10.1007/s10518-013-9496-6.
[22] McKenna F, Scott MH, Fenves GL. Nonlinear finite-element analysis software architecture using object composition. J Comput Civ Eng. 2010;24:95–107. https://doi.org/10.1061/(ASCE)CP.1943-5487.0000002.
[23] O'Reilly GJ, Sullivan TJ. Modeling techniques for the seismic assessment of the existing Italian RC frame structures. J Earthquake Eng 2019;23(8):1262–96. https://doi.org/10.1080/13632469.2017.1360224.
[24] Scott MH, Fenves GL. Plastic hinge integration methods for force-based beam column elements. J Struct Eng 2006;132:244–52. https://doi.org/10.1061/(ASCE)0733-9445(2006) 132:2(244).
[25] Crisafulli FJ, Carr AJ, Park R. Analytical modelling of infilled frame structures – a general review. Bull New Zeal Soc Earthq Eng 2000;33(1):30–47.
[26] Haselton C, Liel A, Taylor S, Deierlein G. Beam-column element model calibrated for predicting flexural response leading to global collapse of RC frame buildings. PEER repost 2007/03; 2008.
[27] Belleri A, Torquati M, Marini A, Riva P. Horizontal cladding panels: in-plane seismic performance in precast concrete buildins. Belletin Earthquake Eng 2016. https://doi.org/10.1007/s10518-015-9861-8.
[28] Lagomarsino S, Penna A, Galasco A, Cattari S. TREMURI program: an equivalent frame model for the nonlinear seismic analysis of masonry buildings. Eng Struct 2013;56:1787–99. https://doi.org/10.1016/j.engstruct.2013.08.002.
[29] Chopra AK, McKenna F. Modeling viscous damping in nonlinear response history analysis of buildings for earthquake excitation. Earthq Eng Struct Dyn 2016;45:193–211. https://doi.org/10.1002/eqe.2622.
[30] O'Reilly GJ, Perrone D, Fox MJ, Lanese I, Monteiro R, Filiatrault A, et al. System identification and seismic assessment modelling implications for Italian school buildings. J Perform Constr Facil 2019.
[31] Montaldo V, Meletti C. Valutazione del valore della ordinata spettrale a 1sec e ad altri periodi di interesse ingegneristico. Progetto DPC-INGV S1, Deliverable D3; 2007.
[32] Meletti C, Galadini F, Valensise G, Stucchi M, Basili R, Barba S, et al. A seismic source zone model for the seismic hazard assessment of the Italian territory. Tectonoph 2008;450:85–108. https://doi.org/10.1016/j.tecto.2008.01.003.
[33] Iervolino I, Chioccarelli E, Cito P. REASSESS V1.0: A computationally efficient software for probabilistic seismic hazard analysis. In: COMPDYN 2015–5th ECCOMAS themat conf comput methods struct dyn earthq Eng, Crete Island, Greece; 2015.
[34] Ancheta TD, Darragh RB, Stewart JP, Seyhan E, Silva WJ, Chiou BSJ, et al. PEER NGA-West2 Database. PEER Rep 2013/03; 2013.
[35] Morandi P, Albanesi L, Graziotti F, Li Piani T, Penna A, Magenes G. Development of a dataset on the in-plane experimental response of URM piers with bricks and blocks. Constr Build Mater 2018;190:593–611. https://doi.org/10.1016/j.conbuildmat.2018.09.070.
[36] EN 1998-3:2005. Eurocode 8: Design of structures for earthquake resistance – Part 3: Assessment and retrofit of buildings. Brussels, Belgium; 2005.
[37] Dolšek M, Fajfar P. Simplified non-linear seismic analysis of infilled reinforced concrete frames. Earthquake Engng Struct. Dyn 2005;34(1):49–66. https://doi.org/10.1002/eqe.411.
[38] Dolšek M, Fajfar P. Inelastic spectra for infilled reinforced concrete frames. Earthquake Engng Struct Dyn 2004;33(15):1395–416. https://doi.org/10.1002/eqe.410.
[39] Tasligedik S, Akguzel U, Kam W, Pampanin S. Strength hierarchy at reinforced concrete beam-column joints and global capacity. J Earthquake Eng 2016:1–34. https://doi.org/10.1080/13632469.2016.1233916.
[40] Galal K, Ghobarah A. Shear capacity of retrofitted rectangular RC short columns. In: 13th world conference on earthquake engineering, Vancouver, B.C., Canada; 2004.
[41] Priestley N, Seible F, Verma R, Xiao Y. Seismic shear strength of reinforced concrete columns," Report SSRP-93/06, San Diego, CA, USA; 1993.
[42] FEMA P695. Quantification of building seismic performance factors. Washington,

DC, USA; 2009.
[43] Baker JW. Efficient analytical fragility function fitting using dynamic structural analysis. Earthq Spectra 2015;31:579–99. https://doi.org/10.1193/021113EQS025M.
[44] O'Reilly GJ, Sullivan TJ, Monteiro R. On the seismic assessment and retrofit of infilled RC frames structures. In: 16th Eur conf earthq Eng, Thessaloniki, Greece; 2018.
[45] ASCE 41-17. Seismic Evaluation and Retrofit of Existing Buildings. American Society of Civil Engineers, Reston, Virginia; 2017.
[46] Rossetto T, Elnashai A. Derivation of vulnerability functions for European-type RC structures based on observational data. Eng Struct 2003;25:1241–63. https://doi.org/10.1016/S0141-0296(03)00060-9.
[47] Rota M, Penna A, Magenes G. A methodology for deriving analytical fragility curves for masonry buildings based on stochastic nonlinear analyses. Eng Struct 2010;32(5):1312–23. https://doi.org/10.1016/j.engstruct.2010.01.009.
[48] O'Reilly GJ, Sullivan TJ. Quantification of modelling uncertainty in existing Italian RC frames. Earthq Eng Struct Dyn 2018;47:1054–74. https://doi.org/10.1002/eqe.3005.
[49] FEMA P58-3. Seismic Performance Assessment of Buildings Volume 3—Performance Assessment Calculation Tool (PACT) Version 2.9.65 (FEMA P-58-3.1). vol. 3. Washington, DC; 2012.
[50] Dolšek M, Lazar Sinković N, Žižmond J. IM-based and EDP-based decision models for the verification of the seismic collapse safety of buildings. Earthq Eng Struct Dyn 2017;46:2665–82. https://doi.org/10.1002/eqe.2923.
[51] Cardone D, Perrone G. Damage and loss assessment of Pre-70 RC frame buildings with FEMA P-58. J Earthq Eng 2017;21:23–61. https://doi.org/10.1080/13632469.2016.1149893.
[52] Perrone G, Cardone D, O'Reilly GJ, Sullivan TJ. Developing a direct approach for estimating expected annual losses of Italian buildings. J Earthquake Eng 2019:1–32. https://doi.org/10.1080/13632469.2019.1657988.
[53] Sousa L, Monteiro R. Seismic retrofit options for non-structural building partition walls: impact on loss estimation and cost-benefit analysis. Eng Struct 2018;161:8–27. https://doi.org/10.1016/j.engstruct.2018.01.028.
[54] Ottonelli D, Cattari S, Lagomarsino S. Assessment and retrofit of masonry structures. In: Sullivan TJ, Calvi GM, Monteiro R, editors. Towar simpl displac loss assess retrofit approaches, Pavia, Italy; 2016. p. 5–62.
[55] Cornali F, Belleri A, Riva P. Assessment and retrofit of pre-cast concrete buildings. In: Sullivan TJ, Calvi GM, Monteiro R, editors. Towar simpl displac loss assess. Retrofit Approaches, Pavia, Italy; 2016. p. 181–221.
[56] Vona M, Masi A. Resistenza sismica di telai in c.a. progettati con il R.D. 2229/39, in XI Congresso Nazionale 'L'Ingegneria Sismica in Italia'. Genova, Italia; 2004.
[57] Holmes T. Risk assessment and retrofit of existing buildings. 12th World congress on earthquake engineering. 2000.
[58] FEMA E-74. Reducing the risk of nonstructural earthquake damage – a practical guide. Washington, DC; 2012.
[59] NIST GCR 17-917-44, Seismic analysis, design, and installation of nonstructural components and systems - background and recommendations for future work; 2017.
[60] Ilki A, Kumbasar N, Koc V. Low strength concrete members externally confined with FRP sheets. Struct Eng Mech 2004;18:1–28. https://doi.org/10.12989/sem.2004.18.2.167.
[61] Marcari G, Manfredi G, Prota A, Pecce M. In-plane shear performance of masonry walls strengthened with FRP. Composites Part B 2007;38(7):887–901. https://doi.org/10.1016/j.compositesb.2006.11.004.
[62] Elnashai AS, Pinho R. Repair and retrofitting of RC walls using selective techniques. J Earthquake Eng 1998;2(4):525–68. https://doi.org/10.1080/13632469809350334.
[63] Del Vecchio C, Di Ludovico M, Prota A, Manfredi G. Analytical model and design approach for FRP strengthening of non-conforming RC corner beam-column joints. Eng Struct 2015;87:8–20. https://doi.org/10.1016/j.engstruct.2015.01.013.
[64] Akguzel U, Pampanin S. Assessment and design procedure for the seismic retrofit of reinforced concrete beam-column joints using FRP composite materials. ASCE J Compos Constr 2012;16(1):21–34.
[65] Mugahed Y, Rayed A, Raizal S, Hisham A, Hunge C. Properties and applications of FRP in strengthening RC structures: a review. Structures 2018;16:208–38. https://doi.org/10.1016/j.istruc.2018.09.008.
[66] Kadid A, Yahiaoui D. Seismic assessment of braced RC frames. Procedia Eng 2011;14:2899–905. https://doi.org/10.1016/j.proeng.2011.07.365.
[67] Massumi A, Tasnimi A. Strengthening of low ductile reinforced concrete frames using steel X-bracings with different details. In: The 14th world conference on earthquake engineering, Beijing, China; 2008.
[68] Di Cesare A, Ponzo F. Seismic retrofit of reinforced concrete frame buildings with hysteretic bracing systems: design procedure and behaviour factor. Shock Vib 2017. https://doi.org/10.1155/2017/2639361.
[69] Lignos DG, Karamanci E, Martin G. A Steel database for modelling post-buckling behavior and fracture of concentrically braced frames under earthquakes. In: 15th world conference on earthquake engineering, Lisbon, Portugal; 2012.
[70] Uriz, P, Mahin, SA. Toward earthquake-resistant design of concentrically braced steel-frame structures. PEER Report 2008/08, Berkeley, California; 2008.
[71] Filippou FC, Popov EP, Bertero VV. Effects of Bond Deterioration on Hysteretic Behavior of Reinforced Concrete Joints. Report EERC 83-19, Earthquake Engineering Research Center, University of California, Berkeley; 1983.
[72] Belleri A, Torquati M, Riva P. Seismic performance of ductile connections between precast beams and roof elements. Mag Concr Res 2013;66(11):553–62. https://doi.org/10.1680/macr.13.00092.
[73] Fib. Structural connections for precast concrete building, guide to good practice. Bulletin 43; 2008.
[74] Bournas DA, Negro P, Taucer F. Performance of industrial buildings during the Emilia earthquakes in Northern Italy and recommendations for their strengthening. Bull Earthq Eng 2014;12:2383–404.
[75] De Stefani L, Scotta R, Lazzari M. Optimal design of seismic retrofitting of RC frames with eccentric steel bracing. Bull Earthquake Eng 2014;13:603. https://doi.org/10.1007/s10518-014-9633-x.
[76] Christopoulos C, Filiatrault A. Principles of passive supplemental damping and seismic isolation. IUSS Press, ISBN: 88-7358-037-8, Pavia, Italy; 2006.
[77] Sismocell – Reglass H.T. S.r.l. Sistema antisismico Sismocell; 2020. Available online at: https://sismocell.com/dispositivo-antisismico [in Italian].
[78] CNR-DT 200 R1/2013. Consiglio nazionale delle ricerche. Istruzioni per la progettazione, l'esecuzione ed il controllo di interventi di consolidamento statico mediante l'utilizzo di compositi fibrorinforzati.
[79] Gaetani d'Aragona M, Polese M, Di Ludovico M, Prota A. Seismic vulnerability for RC infilled frames: simplified evaluation for as-built and retrofitted building typologies. Buildings 2018;8(10):137. https://doi.org/10.3390/buildings8100137.
[80] Caterino N, Iervolino I, Manfredi G, Cosenza E. Multi-criteria decision making for seismic retrofitting of RC structures. J Earthquake Eng 2008;12:555–83. https://doi.org/10.1080/13632460701572872.
[81] CPE Candidate No. 0115808. How to estimate the cost of different structural beam and column connections (comparison); 2015.
[82] Cosenza E, Del Vecchio C, Di Ludovico M, Dolce M, Moroni C, Prota A, et al. The Italian guidelines for seismic risk classification of constructions: technical principles and validation. Bull Earthq Eng 2018;16:5905–35. https://doi.org/10.1007/s10518-018-0431-8.